Eur. Phys. J. B **76**, 565–580 (2010)
DOI: 10.1140/epjb/e2010-00227-x

THE EUROPEAN PHYSICAL JOURNAL B

Regular Article

Conservative bounds on Rayleigh-Bénard convection with mixed thermal boundary conditions

R.W. Wittenberg[a] and J. Gao[b]

Department of Mathematics, Simon Fraser University, Burnaby, BC V5A 1S6, Canada

Received 20 April 2010
Published online 20 July 2010 –

Abstract. Using the background field variational method developed by Doering and Constantin, we obtain upper bounds on heat transport in Rayleigh-Bénard convection assuming mixed (Robin) thermal conditions of arbitrary Biot number η at the fluid boundaries, ranging from the fixed temperature (perfectly conducting, $\eta = 0$) to the fixed flux (perfectly insulating, $\eta = \infty$) extremes. Solving the associated Euler-Lagrange equations, we numerically find optimal bounds on the averaged convective heat transport, measured by the Nusselt number Nu, over a restricted one-parameter class of piecewise linear background temperature profiles, and compare these to conservative analytical bounds derived using elementary functional estimates. We find that analytical estimates fully capture the scaling behaviour of the semi-optimal numerical bounds, including a clear transition from fixed temperature to fixed flux behaviour observed for any small nonzero η as the usual Rayleigh number Ra increases, suggesting that in the strong driving limit, all imperfectly conducting boundaries effectively act as insulators. The overall bounds, optimized over piecewise linear backgrounds, are $Nu \leq 0.045\, Ra^{1/2}$ in the fixed temperature case $\eta = 0$, and $Nu \leq 0.078\, Ra^{1/2}$ in the large-Ra limit in all other cases, $0 < \eta \leq \infty$.

1 Introduction

Thermal convection, in which heating from below and cooling from above induces buoyancy-driven flow in a fluid, has long attracted considerable research interest, both for the fascinating scientific problems it presents and due to its wide-ranging relevance to the earth and astrophysical sciences, engineering and elsewhere. A common paradigm for this research is the behaviour of the Rayleigh-Bénard model system, in which a fluid layer sandwiched between two horizontal plates is subject to thermal driving; and much attention has focused on the dynamical and statistical properties of the turbulent state attained for sufficiently strong heating [1,2]. Despite intensive experimental and theoretical efforts, some fundamental problems in turbulent convection remain incompletely understood, however, such as the scaling of the Nusselt number Nu, representing the convective enhancement of vertical heat transport, with the Rayleigh number Ra, a measure of the driving via the temperature difference across the fluid layer [3].

While a detailed analytical understanding of solutions of the governing fluid equations is beyond reach, there has been considerable success in finding a priori bounds on time-averaged bulk flow quantities using energy balances derived from the Navier-Stokes equations. Inspired by suggestions of Malkus [4], the "optimum theory of turbulence" of Howard [5,6] and Busse [7,8] was the first systematic approach to obtaining such bounds, via variational principles derived under statistical stationarity assumptions, and continues to be of interest [9]. More recently, the "background method" of Doering and Constantin (based on a decomposition introduced by Hopf [10]), has allowed rigorous upper bounds to be proved without requiring assumptions on the flow; initially developed for shear flows [11,12], it has subsequently been fruitfully applied to numerous contexts in convection [13] and elsewhere, and is the approach taken in the present study. When both approaches are applicable, the optimal bounds obtained in the Malkus-Howard-Busse (MHB) and Constantin-Doering-Hopf (CDH) methods can be shown to coincide [14–16].

The background method for convection relies on the decomposition of the physical temperature field $T(\mathbf{x}, t)$ into a "background" profile $\tau(z)$, which satisfies the inhomogeneous applied thermal boundary conditions (BCs), and a "fluctuation field" $\theta(\mathbf{x}, t)$ (decompositions with a nonzero background velocity or a more general temperature background appear not to improve the bounds [15]). The upper bound on Nu can be expressed as a functional of the background field τ, and is usually expressed in the final form $Nu \leq CRa^p$ (up to a possible logarithmic Ra-dependence), where in general both the exponent p and the prefactor C are expected to depend on τ.

[a] e-mail: ralf@sfu.ca
[b] *Current address*: QuIC Financial Technologies, Suite 1105, 1095 W. Pender St., Vancouver, BC V6E 2M6, Canada.

The problem of finding the optimal (lowest) upper bound then becomes one of minimizing this functional, subject to a positivity condition on a τ-dependent quadratic form, or equivalently, a "spectral condition" on an associated linear functional. The analytical solution of the full variational problem for the optimal background profile, incorporating the spectral constraint, is in general out of reach except in simplified cases (see [17] and [18, Chap. 2]); whereas the complete numerical solution of the CDH variational upper bounding problem, while achievable [19,20], requires extensive careful and delicate computations.

Instead of attempting to solve the full optimal problem over all backgrounds, conservative (non-optimal) bounds may more readily be obtained by restricting consideration to parametrized families of background profiles $\tau_{(\mathbf{p})}(z)$; the spectral constraint then translates to conditions on the parameter(s) $\mathbf{p}$. Given explicit formulas for $\tau_{(\mathbf{p})}(z)$, in many cases functional estimates applied directly to the quadratic form can be used to derive sufficient conditions on $\mathbf{p}$ for satisfaction of the spectral constraint, and hence to obtain rigorous, fully analytical bounds on the *Nu*-*Ra* relationship.

The simplest and most common choice is to let the background profiles $\tau = \tau_\delta(z)$ be piecewise linear functions parametrized by a boundary layer width δ, with $\tau' = 0$ in the bulk of the domain. With this choice elementary, uniform in wave number Cauchy-Schwarz estimates on the quadratic form often suffice to establish analytical bounds $Nu \leq CRa^p$. In some cases, the scaling exponent p in these bounds is already optimal (by comparison with more careful analyses and/or experimental expectations), so that improvements achieved through optimization over a wider class of backgrounds τ or more careful verification of the spectral constraint could at best lower the prefactor C in the bound. Notably, for finite Prandtl number convection with fixed temperature BCs, the analytical exponent $p = 1/2$ proved using piecewise linear backgrounds in the pioneering work of Doering and Constantin [13] coincides with that obtained in the full optimal solution of the bounding problem [19].

Given the apparent crudeness of the derivation of such analytical bounds, in general one may wonder whether a scaling exponent p obtained in this way is the best possible, even within the restricted one-parameter family of piecewise linear background profiles $\tau_\delta(z)$. Otero [18] has developed a semi-analytic method for computing the optimal bound on the *Nu*-*Ra* relationship over all backgrounds $\tau_\delta(z)$, combining exact solutions of the (piecewise constant coefficient) Euler-Lagrange equations for the minimizing fields with numerical solution of the nonlinear algebraic equations enforcing solvability (for each horizontal wave number separately), and overall numerical optimization. In the cases in which a comparison has been performed to date – shear flow (compare [12] with [18]), infinite Prandtl number convection [18,21], and porous medium flow [22,23] – the conservative analytical estimates have been found to capture the scaling optimized available over all piecewise linear backgrounds $\tau_\delta(z)$. In the present work, we compare scaling behaviours predicted by the elementary estimates to the semi-optimal results obtained using Otero's method in some detail, for the overall *Nu*-*Ra* bound but also vis-à-vis intermediate quantities and the behaviour of the balance parameter [24].

In studies of turbulent Rayleigh-Bénard convection, a common assumption – as in the analyses cited above – is that the lower and upper boundaries of the fluid are held at known uniform temperature, or equivalently, that the bounding plates are perfect conductors. Realistically, though, boundaries are imperfectly conducting; and even when they have much higher conductivity than the fluid, as is typical, as Ra (and hence Nu) increases, the Nu-dependent *effective* conductivity of the fluid eventually becomes comparable to and then exceeds that of the plates. In fact, in the $Ra \to \infty$ limit one might expect the fluid effectively to "short circuit" the system, with the bounding plates acting essentially as perfect insulators by comparison; in this extreme it would be the *heat flux*, rather than the *temperature*, which is fixed at the boundaries.

Motivated by such considerations, Otero et al. [25] showed that the CDH background method could be used to obtain upper bounds on convective heat transport also in the limiting case of fixed flux BCs, as discussed further below. In the last decade various modelling [26,27], experimental [28] and numerical [29] studies have also sought to understand the effect on heat transport of the thermal properties of the boundaries, and the finite thermal conductivity of the bounding plates is now commonly taken into account in interpreting experiments [3,30,31]. In this light, it is notable that recent extensive investigations using direct numerical simulation [32–34] have, rather surprisingly, found no apparent difference in the *Nu*-*Ra* relationship between fixed temperature and fixed flux thermal BCs.

The above-mentioned analysis of Otero et al. [25] on finite Prandtl number, fixed flux convection, using the standard background fields $\tau_\delta(z)$ and elementary functional estimates on the quadratic form, demonstrated an upper bound of the form $Nu \leq C_\infty Ra^{1/2}$. While the overall scaling exponent $p = 1/2$ agreed with that previously obtained for fixed temperature BCs (albeit with a slightly different prefactor, $C_\infty \neq C_0$), the intermediate estimates underlying these bounds were quite different. In particular, since for fixed heat flux the (averaged) temperature drop across the fluid is not known a priori, it was necessary to introduce a control parameter R as a measure of the driving, and the overall bound was found via estimates of the form $Nu \leq \widetilde{c}\, R^{1/3}$, $Ra \geq \widetilde{c}'\, R^{2/3}$ [25].

In recent work by one of us [35], the bounding formalism for finite Prandtl number Rayleigh-Bénard convection was developed for general mixed thermal BCs with fixed Biot number η, identifying the fixed temperature [13] and fixed flux [25] bounding problems as the $\eta = 0$ and $\eta = \infty$ extremes of the general case.

In this paper we consider the bounding problem for general Biot number η in more depth. We review the formulation [35], describe the spectral constraint on background profiles $\tau(z)$, and discuss analytical bounds for

piecewise linear profiles $\tau_\delta(z)$. We also describe Otero's method [16,18,23] and use it to compute the optimal solution of the full variational problem over backgrounds $\tau_\delta(z)$; again, the overall bounds have the form $Nu \leq C_\eta Ra^{1/2}$, where our computed prefactors improve on previous results for the fixed flux and general Biot number cases $0 < \eta \leq \infty$. As in [18,23], we find that the wave number-independent elementary analytical estimates yield the optimal scaling available for backgrounds of the form $\tau_\delta(z)$; this agreement extends also to intermediate scaling behaviours and the balance parameter. In particular, for small η the numerical semi-optimal bounds show a clear transition from a fixed temperature to a fixed flux scaling regime as Ra increases, as predicted analytically [35]; we find $C_\eta = C_\infty$ for all $\eta > 0$.

2 Formulation of equations

We begin by summarizing the governing equations and identities; see [35] for more details.

2.1 Fluid equations

Consider a fluid of density ρ_f, kinematic viscosity ν_f, thermal diffusivity κ_f and thermal expansion coefficient α confined between two horizontal parallel plates, separated by a distance h (and let the gravitational acceleration be $-g\,\mathbf{e_z}$). At the upper and lower boundaries of the fluid (the interfaces with the bounding plates, assumed to have identical thermal properties), thermal driving is applied, with the thermal boundary conditions (BCs) assumed to take the general mixed (Robin) form $T^* + \eta^* \mathbf{n}\cdot\nabla T^* = A^*_{l,u}$ at $z = 0, h$ for some given A^*_l and $A^*_u < A^*_l$ (for $0 \leq \eta^* < \infty$; variables with stars are dimensional). These BCs imply a temperature scale Θ and reference temperature $T_{\rm ref}$,

$$\Theta = \frac{A^*_l - A^*_u}{1 + 2\eta^*/h}, \qquad T_{\rm ref} = \frac{A^*_u + \eta^*(A^*_l + A^*_u)/h}{1 + 2\eta^*/h}, \quad (2.1)$$

chosen so that the conduction temperature profile takes the dimensionless form $T = 1 - z$ across the fluid [35].

The dimensionless fluid equations, in the Boussinesq approximation, for the velocity field $\mathbf{u} = u\,\mathbf{e_x} + v\,\mathbf{e_y} + w\,\mathbf{e_z}$ and temperature field T take the form

$$Pr^{-1}\left(\frac{\partial \mathbf{u}}{\partial t} + \mathbf{u}\cdot\boldsymbol{\nabla}\mathbf{u}\right) + \boldsymbol{\nabla} p = \nabla^2\mathbf{u} + R\,T\,\mathbf{e_z}, \quad (2.2)$$

$$\boldsymbol{\nabla}\cdot\mathbf{u} = 0, \quad (2.3)$$

$$\frac{\partial T}{\partial t} + \mathbf{u}\cdot\boldsymbol{\nabla} T = \nabla^2 T \quad (2.4)$$

in the fluid $0 < z < 1$, where we nondimensionalized with respect to the fluid layer thickness h, thermal diffusivity time h^2/κ_f and temperature scale Θ. We assume L_x, L_y-periodicity in all variables in the horizontal x- and y-directions, respectively; and the velocity field satisfies the usual no-slip BCs $\mathbf{u} = \mathbf{0}$ at $z = 0, 1$.

In dimensionless form, the mixed (Robin) thermal BCs take the form

$$T - \eta\,T_z = 1 + \eta \ \text{ on } \ z = 0, \quad T + \eta\,T_z = -\eta \ \text{ on } \ z = 1, \quad (2.5)$$

where $\eta = \eta^*/h$ is the *Biot number*. The limiting cases are well-understood: for $\eta \to 0$, (2.5) reduces to the *fixed temperature* (Dirichlet) thermal BCs

$$T = 1 \ \text{ on } \ z = 0, \qquad T = 0 \ \text{ on } \ z = 1, \quad (2.6)$$

while $\eta \to \infty$ gives the *fixed flux* (Neumann) limit

$$T_z = -1 \ \text{ on } \ z = 0 \text{ and } z = 1. \quad (2.7)$$

In (2.2), Pr is the usual Prandtl number $Pr = \nu_f/\kappa_f$, while the other dimensionless parameter R is the *control parameter* for the system. Since the actual temperature drop across the fluid is given directly by the thermal BCs only in the fixed temperature case $\eta = 0$, in lieu of the usual Rayleigh number R is defined in terms of the temperature scale Θ from (2.1) as

$$R = \frac{\alpha g h^3}{\nu_f \kappa_f}\,\Theta\,. \quad (2.8)$$

2.1.1 Notation

As in [25], we define the horizontal average of functions $h(\mathbf{x}) = h(x, y, z)$ as

$$\overline{h}(z) = \frac{1}{A}\int_0^{L_y}\int_0^{L_x} h(x, y, z)\,dxdy,$$

where $A = L_x L_y$ is the dimensionless cross-sectional area, and the time average of functions $g(t)$ by

$$\langle g\rangle = \limsup_{\tau\to\infty}\frac{1}{\tau}\int_0^\tau g(t)\,dt.$$

The notation $\int_f h = A\int_0^1 \overline{h}(z)\,dz$ denotes a volume integral over the entire fluid layer, and L^2 norms are defined over the fluid in the usual way:

$$\|h\|^2 = \int_f h^2 = \int_0^1\int_0^{L_y}\int_0^{L_x} h^2(x, y, z)\,dxdy\,dz.$$

2.2 Rayleigh and Nusselt numbers

The physical *temperature drop* across the fluid, averaged horizontally and over time, is $\Delta T^* = \langle \overline{T^*}|_{z^*=0} - \overline{T^*}|_{z^*=h}\rangle$, or in nondimensional form,

$$\Delta T = -\langle \overline{T}\big|_{z=0}^1\rangle = \langle \overline{T}|_{z=0} - \overline{T}|_{z=1}\rangle = \frac{\Delta T^*}{\Theta}, \quad (2.9)$$

in the fixed temperature case $\eta = 0$ we have $\Delta T^* = \Theta$, $\Delta T = 1$, but in general this is unknown *a priori*. One may readily verify that in equilibrium, the heat fluxes across

the bottom and top boundaries of the fluid balance, and we define the horizontally- and time-averaged nondimensional *boundary heat flux* as

$$\beta = \langle -\overline{T}_z \rangle\big|_{z=0} = \langle -\overline{T}_z \rangle\big|_{z=1}, \tag{2.10}$$

this is fixed at $\beta = 1$ (only) for fixed flux BCs $\eta = \infty$. For $0 < \eta < \infty$, the fixed Biot number BCs (2.5) immediately imply a relation between ΔT and β:

$$\Delta T + 2\eta\,\beta = 1 + 2\eta. \tag{2.11}$$

The usual *Rayleigh number* Ra, defined in terms of the (averaged) temperature drop across the fluid, is now related to the control parameter R via

$$Ra = \frac{\alpha g h^3}{\nu_f \kappa_f} \Delta T^* = R\,\Delta T. \tag{2.12}$$

The *Nusselt number*, the ratio of the total to the conductive vertical heat transport, may be computed as usual via $Nu = 1 + \langle \int_f wT \rangle / A\,\Delta T$. Now $\langle \int_f wT \rangle$ may be evaluated via averages of the thermal advection-diffusion equation (2.4), to give the general Nusselt number identity [35]

$$Nu = \frac{\beta}{\Delta T}, \tag{2.13}$$

from which, using (2.12), we obtain $Nu\,Ra = R\,\beta$. Note that, for $0 < \eta < \infty$, to obtain an upper bound on Nu it is sufficient to bound *either* β from above *or* ΔT from below, since ΔT and β are related by (2.11).

2.2.1 Energy identities

Taking the inner product of (2.2) with $\mathbf{u}$, integrating over the fluid using incompressibility and the boundary conditions, and taking time averages gives the expression for the momentum dissipation

$$\frac{1}{AR} \langle \|\boldsymbol{\nabla} \mathbf{u}\|^2 \rangle = \frac{1}{A} \left\langle \int_f wT \right\rangle = \beta - \Delta T, \tag{2.14}$$

note that this implies $Nu = \beta/\Delta T \geq 1$. Similarly, we obtain the thermal energy identity by multiplying (2.4) by T, integrating by parts and time averaging, to give

$$\frac{1}{A} \langle \|\boldsymbol{\nabla} T\|^2 \rangle = \left\langle \overline{TT_z}\big|_{z=0}^1 \right\rangle. \tag{2.15}$$

2.3 Background field

Following the Constantin-Doering-Hopf "background" approach, we decompose the velocity and temperature fields into "background" and "fluctuating" fields, via $\mathbf{u}(\mathbf{x}, t) = \mathbf{0} + \mathbf{v}(\mathbf{x}, t)$ (using zero background velocity) and

$$T(\mathbf{x}, t) = \tau(z) + \theta(\mathbf{x}, t). \tag{2.16}$$

Here the background temperature profile $\tau(z)$ carries the inhomogeneous BCs (2.5), $\tau(0) - \eta\tau'(0) = 1 + \eta$ and $\tau(1) + \eta\tau'(1) = -\eta$, so that $\theta(\mathbf{x}, t)$ satisfies homogeneous Robin BCs with fixed Biot number, $\theta + \eta \mathbf{n} \cdot \nabla\theta = 0$, or in our geometry,

$$\theta - \eta\,\theta_z = 0 \quad \text{at} \quad z = 0, \qquad \theta + \eta\,\theta_z = 0 \quad \text{at} \quad z = 1. \tag{2.17}$$

Defining $\Delta\tau = \tau(0) - \tau(1)$, $\gamma = -\tau'(0) = -\tau'(1)$, the BCs on $\tau(z)$ imply the relation (compare (2.11))

$$\Delta\tau + 2\eta\,\gamma = 1 + 2\eta. \tag{2.18}$$

Substituting the decomposition (2.16) into (2.2)–(2.4), we obtain the evolution equations for the velocity and temperature fluctuations,

$$Pr^{-1} \left(\frac{\partial \mathbf{v}}{\partial t} + \mathbf{v} \cdot \boldsymbol{\nabla} \mathbf{v} \right) + \boldsymbol{\nabla} \tilde{p} = \nabla^2 \mathbf{v} + R\,\theta\,\mathbf{e_z}, \tag{2.19}$$

$$\frac{\partial \theta}{\partial t} + \mathbf{v} \cdot \boldsymbol{\nabla} \theta = \nabla^2 \theta + \tau'' - w\tau', \tag{2.20}$$

with $\boldsymbol{\nabla} \cdot \mathbf{v} = 0$, where the $R\,\tau\,\mathbf{e_z}$ term has been absorbed into a redefined pressure. Multiplying (2.19) and (2.20) by $\mathbf{v}$ and θ, respectively, and integrating over the domain, we find that norms of the fluctuations evolve according to

$$\frac{1}{2PrR} \frac{d}{dt} \|\mathbf{v}\|^2 = -\frac{1}{R} \|\boldsymbol{\nabla} \mathbf{v}\|^2 + \int_f w\theta, \tag{2.21}$$

$$\frac{1}{2} \frac{d}{dt} \|\theta\|^2 = -\|\boldsymbol{\nabla}\theta\|^2 + A\,\overline{\theta\theta_z}\big|_{z=0}^1 - \int_f \theta_z \tau' + A\,\overline{\theta}\tau'\big|_{z=0}^1 - \int_f w\theta\tau'. \tag{2.22}$$

2.3.1 An identity for the boundary heat flux β

As preparation for formulating a variational bounding principle, we obtain an identity giving β as a sum of a functional of the background τ and a τ-dependent quadratic form in the fluctuating fields $\mathbf{v}$ and θ. We outline the derivation of such a formula; see [35] for more details.

We relate the norms of gradients of the fields $\mathbf{u}$ and T (which are related to β and ΔT through (2.14)–(2.15)) to those of $\mathbf{v}$ and θ by expressing the decomposition $\mathbf{u} = \mathbf{v}$, $T = \tau + \theta$ in the form

$$\frac{1}{R} \|\boldsymbol{\nabla} \mathbf{u}\|^2 = \frac{1}{R} \|\boldsymbol{\nabla} \mathbf{v}\|^2, \tag{2.23}$$

$$\|\boldsymbol{\nabla} T\|^2 = \|\boldsymbol{\nabla}\theta\|^2 + 2 \int_f \theta_z \tau' + \int_f \tau'^2. \tag{2.24}$$

Introducing a "balance parameter" b [24], we form the combination $b[2(2.22) + (2.24)] + (1 - b)[(2.23)]$; taking time averages and substituting (2.14)–(2.15), we find

$$bA\langle \overline{TT_z}\big|_{z=0}^1 \rangle + (1-b)A(\beta - \Delta T) = b \int_f \tau'^2 + 2bA \left\langle \overline{\theta\theta_z}\big|_{z=0}^1 + \overline{\theta}\tau'\big|_{z=0}^1 \right\rangle - b\,\mathcal{Q}_{\tau, R_e}[\mathbf{v}, \theta]. \tag{2.25}$$

Here we have defined the quadratic form $\mathcal{Q}_{\tau,R_e}$ by

$$\mathcal{Q}_{\tau,R_e}[\mathbf{v},\theta] = \left\langle \int_f \left[\frac{1}{R_e}|\boldsymbol{\nabla}\mathbf{v}|^2 + 2\tau' w\theta + |\boldsymbol{\nabla}\theta|^2 \right] \right\rangle, \tag{2.26}$$

where for $b > 1$ the *"effective control parameter"* R_e is

$$R_e = \frac{b}{b-1}R \geq R. \tag{2.27}$$

Simplifying the first term in (2.25) using (2.16) and rearranging terms, we obtain

$$b\,(\beta\Delta\tau - \gamma\Delta T) + (1-b)(\beta - \Delta T) = b\left(\int_0^1 \tau'^2\,dz - \gamma\Delta\tau\right) - \frac{b}{A}\mathcal{Q}'_{\tau,R_e}[\mathbf{v},\theta], \tag{2.28}$$

where the modified quadratic form $\mathcal{Q}'_{\tau,R_e}$ is

$$\mathcal{Q}'_{\tau,R_e}[\mathbf{v},\theta] = \mathcal{Q}_{\tau,R_e}[\mathbf{v},\theta] - A\left\langle \overline{\theta\theta_z}\big|_{z=0}^1 \right\rangle; \tag{2.29}$$

note that the added boundary term vanishes in both the fixed temperature and fixed flux limits. For mixed thermal BCs with finite Biot number, we may now substitute for ΔT and $\Delta\tau$ using (2.11) and (2.18), to obtain an identity purely in terms of β and γ; after some algebra, this is

$$(1+2\eta)(\beta - 1) = b\left(\int_0^1 \tau'^2\,dz - (1+2\eta) + 2\eta\gamma^2\right) - \frac{b}{A}\mathcal{Q}'_{\tau,R_e}[\mathbf{v},\theta], \tag{2.30}$$

where for fixed $\eta < \infty$, the boundary term in $\mathcal{Q}'_{\tau,R_e}$ from (2.29) can be written, using (2.17), as

$$\overline{\theta\theta_z}\big|_{z=0}^1 = -\eta\left(\overline{\theta_z^2}|_{z=0} + \overline{\theta_z^2}|_{z=1}\right) \leq 0. \tag{2.31}$$

3 A bounding principle

The identity (2.30) now forms the basis for finding an upper bound on β and hence (via (2.11) and (2.13)) on the Nusselt number Nu: let the class of *allowed* fields be those scalar fields $\theta(\mathbf{x})$ and divergence-free vector fields $\mathbf{v}(\mathbf{x})$ satisfying the homogeneous BCs of the problem, namely horizontal periodicity, the no-slip condition $\mathbf{v} = \mathbf{0}$ on $z = 0$, 1, and conditions (2.17) on θ; note that the class of allowed fields in this sense includes all solutions of (2.19)–(2.20) at each time t. Then if for all allowed $\mathbf{v}$ and θ, $\mathcal{Q}'_{\tau,R_e}[\mathbf{v},\theta]$ is bounded below, it follows that (2.30) implies an upper bound on β; note that since $\mathcal{Q}'_{\tau,R_e}[\mu\,\mathbf{v},\mu\,\theta] = \mu^2\mathcal{Q}'_{\tau,R_e}[\mathbf{v},\theta]$ for $\mu \in \mathbb{R}$, if the lower bound exists, it must be zero.

Within the CDH background formalism, a bounding principle is thus as follows: if for a given $R > 0$, we can find a background profile $\tau(z)$ and a balance parameter $b > 1$ so that $\mathcal{Q}'_{\tau,R_e}[\mathbf{v},\theta] \geq 0$ for all allowed $\mathbf{v}$ and θ, then (for $\eta < \infty$) an upper bound $\mathcal{B}_\eta$ on the averaged boundary heat flux β is given by

$$\beta \leq 1 - b + \frac{b}{1+2\eta}\left(\int_0^1 \tau'^2\,dz + 2\eta\gamma^2\right) \equiv \mathcal{B}_\eta[\tau;b]. \tag{3.1}$$

Using (2.11) and (2.18), for $\eta > 0$ we may derive the corresponding lower bound $\mathcal{D}_\eta$ for the averaged temperature drop across the fluid ΔT:

$$\Delta T \geq 1 + b(2\Delta\tau - 1) - b\,\frac{2\eta}{1+2\eta}\left(\int_0^1 \tau'^2\,dz + \frac{1}{2\eta}\Delta\tau^2\right) \equiv \mathcal{D}_\eta[\tau;b], \tag{3.2}$$

with $\mathcal{D}_\eta[\tau;b] + 2\eta\,\mathcal{B}_\eta[\tau;b] = 1 + 2\eta$. Consequently, via (2.13) the Nusselt number is bounded above by

$$Nu \leq \mathcal{N}_\eta[\tau;b] = \mathcal{B}_\eta[\tau;b]/\mathcal{D}_\eta[\tau;b]. \tag{3.3}$$

3.1 Admissible backgrounds and the spectral constraint

The requirement that the quadratic form $\mathcal{Q}'_{\tau,R_e}$ is positive semi-definite is a condition on τ: we say that a background field $\tau(z)$ satisfying the inhomogeneous thermal BCs (2.5) is *admissible* for a given $R_e = bR/(b-1) > 0$ (that is, for $R > 0$ and $b > 1$) if $\mathcal{Q}'_{\tau,R_e}[\mathbf{v},\theta] \geq 0$ for all allowed fields $\mathbf{v}$ and θ.

The positivity condition on $\mathcal{Q}'_{\tau,R_e}$ is equivalent to

$$\bar{\lambda}[\tau;R_e] = \inf_{\mathbf{v},\theta} \mathcal{Q}'_{\tau,R_e}[\mathbf{v},\theta] \geq 0, \tag{3.4}$$

where the infimum is taken over allowed fields $\mathbf{v}$ and θ subject to the normalization condition $\|\theta\|^2 + (PrR_e)^{-1}\|\mathbf{v}\|^2 = 1$. This may also be expressed as the condition that the elliptic operator $\mathcal{L}_{\tau,R_e}$ associated with the quadratic form $\mathcal{Q}'_{\tau,R_e}$ has a positive semi-definite spectrum, that is, that the lowest eigenvalue $\lambda^0 = \lambda^0[\tau;R_e]$ of $\mathcal{L}_{\tau,R_e}$ is nonnegative (one may verify using standard methods that $\lambda^0 = \bar{\lambda}$). Consequently, the admissibility criterion on background fields $\tau(z)$ is also referred to as a *spectral constraint* on τ [13].

The Euler-Lagrange equations for the minimization problem in (3.4), giving the eigenvalues λ of $\mathcal{L}_{\tau,R_e}$, are

$$\frac{1}{2}\boldsymbol{\nabla}P - \frac{1}{R_e}\nabla^2\mathbf{v} + \tau'\theta\,\mathbf{e_z} = \frac{\lambda}{PrR_e}\mathbf{v}, \tag{3.5}$$

$$\nabla\cdot\mathbf{v} = 0, \tag{3.6}$$

$$\tau' w - \nabla^2\theta = \lambda\,\theta, \tag{3.7}$$

where $P = P(\mathbf{x})$ and λ are the Lagrange multipliers enforcing the pointwise divergence-free constraint and the normalization condition, respectively. In deriving (3.5)–(3.7), as usual one computes functional derivatives of the quadratic form

$$\mathcal{H}[\mathbf{v},\theta] = \mathcal{Q}'_{\tau,R_e}[\mathbf{v},\theta] - \int_f \left[\lambda\left(|\theta|^2 + \frac{1}{PrR_e}|\mathbf{v}|^2\right) - P\nabla\cdot\mathbf{v}\right],$$

we remark that in calculating $\delta\mathcal{H}/\delta\theta$, the boundary terms obtained from integration by parts cancel exactly with the boundary term in the definition (2.29) of $\mathcal{Q}'_{\tau,R_e}$, indicating that for general Biot number $0 < \eta < \infty$, the retention of the term $A\,\overline{\theta\theta_z}\big|_{z=0}^{1}$ in the quadratic form is crucial.

3.1.1 Stability of the conduction state

We recall the energy, or nonlinear, stability theory of the conduction state $\mathbf{u} = \mathbf{0}$, $T = \tau_c(z) = 1 - z$ for general Biot number $\eta \in [0, \infty]$ [36]: adding (2.21) and (2.22) and substituting $\tau' = -1$, the evolution of arbitrary perturbations from the conduction state satisfies

$$\frac{1}{2}\frac{d}{dt}\left(\frac{1}{PrR}\|\mathbf{v}\|^2 + \|\theta\|^2\right) = -\mathcal{I}[\mathbf{v},\theta], \tag{3.8}$$

where we define the quadratic form

$$\mathcal{I}[\mathbf{v},\theta] = \int_f \left[\frac{1}{R}|\boldsymbol{\nabla}\mathbf{v}|^2 - 2w\theta + |\boldsymbol{\nabla}\theta|^2\right] - A\,\overline{\theta\theta_z}\big|_{z=0}^{1}.$$

Letting $f(t) = \|\theta\|^2 + (PrR)^{-1}\|\mathbf{v}\|^2$, we define

$$\mu_0 = \mu_0(R) = \inf_{\substack{\mathbf{v},\theta \\ f(t)=1}} \mathcal{I}[\mathbf{v},\theta] = \inf_{\substack{\mathbf{v},\theta \\ f(t)\neq 0}} \frac{\mathcal{I}[\mathbf{v},\theta]}{f(t)}, \tag{3.9}$$

where we minimize over allowed fields $\mathbf{v}$ and θ. Then from (3.8) we have $df/dt = -2\mathcal{I}[\mathbf{v},\theta] \le -2\mu_0 f$, so that if $\mu_0 > 0$ for a given R and η, the L^2 norms of all perturbations decay in time, and the conduction solution is stable. Since μ_0 decreases monotonically in R, for each Biot number η there is a critical value $Ra_{c,\eta}$ [37], with $\mu_0(Ra_{c,\eta}) = 0$ (noting that in the conduction state, $\Delta T = 1$ and $R = Ra$), so that for $R < Ra_{c,\eta}$ the conduction state is energy stable and thus the unique time-asymptotic state of the system.

The Euler-Lagrange equations for the fields that minimize $\mathcal{I}[\mathbf{v},\theta]$ are, as usual (with Lagrange multipliers μ and $\pi(\mathbf{x})$ enforcing normalization and incompressibility, respectively),

$$-\frac{R}{2}\boldsymbol{\nabla}\pi + \nabla^2\mathbf{v} + R\,\theta\mathbf{e_z} = -\frac{\mu}{Pr}\mathbf{v}, \tag{3.10}$$

$$\nabla\cdot\mathbf{v} = 0, \tag{3.11}$$

$$\nabla^2\theta + w = -\mu\,\theta, \tag{3.12}$$

with the appropriate homogeneous BCs. These are in fact the same equations as those obtained from (2.19)–(2.20) for the linear stability problem for the conductive state (identifying $R\pi/2$ and p), confirming that the linear and nonlinear stability boundaries coincide in this case.

Since $\mathcal{I}[\mathbf{v},\theta] = \mathcal{Q}'_{\tau_c,R}[\mathbf{v},\theta]$ for stationary fields, comparing (3.5)–(3.7) with (3.10)–(3.12) it is now apparent that the stability of the conduction state $\tau_c(z) = 1 - z$ is equivalent to the admissibility of the background $\tau = \tau_c$ (with R instead of R_e). (We can analogously interpret the spectral constraint for a general background τ as an energy stability criterion on $T = \tau(z)$ at control parameter R_e, *if* it were a solution (with $\mathbf{u} = \mathbf{0}$) of the governing PDEs (2.2)–(2.4)).

For general $R_e = bR/(b-1)$, it follows that the conduction temperature profile $\tau_c(z)$ is admissible for all $R_e \le Ra_{c,\eta}$; whenever this is the case, the bounds in (3.1)–(3.2) are $\mathcal{B}_\eta = \mathcal{D}_\eta = 1$, and the (bound $\mathcal{N}_\eta$ on the) Nusselt number takes its minimum value of 1. Following [24] we may thus determine the largest $R = (b-1)R_e/b$ for which τ_c is admissible, by maximizing $(b-1)Ra_{c,\eta}/b$ over $b > 1$; taking $b = \infty$, so that $R_e = R$, we find that the conduction state is admissible right up to the energy stability boundary $R = Ra_{c,\eta}$. As in [23,24], the use of a balance parameter b permits us to obtain upper bounds bifurcating at the correct value of Ra.

When $R > Ra_{c,\eta}$, the conduction state is unstable, and correspondingly the profile $\tau = \tau_c$ is not admissible for any $b > 1$. In this case, the best bound on the Nusselt number available in this formalism may be obtained, in principle, by minimizing $\mathcal{N}_\eta[\tau; b]$ given in (3.1)–(3.3) over all backgrounds $\tau(z)$ for which $\lambda^0[\tau; R_e] \ge 0$, and over $b > 1$. Now it may be shown (see [13,22]) that for each $R_e > Ra_{c,\eta}$ the set of admissible profiles is convex, and the analytical results outlined below and in [35] show that it is nonempty; it follows that the optimal profile $\tau_{\rm opt}(z)$ minimizing the bound for a given R_e lies on the boundary of this set, with $\lambda^0[\tau_{\rm opt}; R_e] = 0$.

3.2 The spectral constraint in Fourier space

Using horizontal periodicity with periods L_x and L_y in the x- and y-directions, we may Fourier decompose the temperature fluctuation field θ as

$$\theta(x,y,z) = \sum_{\mathbf{k}} e^{\mathrm{i}(k_x x + k_y y)}\hat{\theta}_{\mathbf{k}}(z), \tag{3.13}$$

and similarly for P and the components (u,v,w) of $\mathbf{v}$, where $\mathbf{k} = (k_x, k_y) = (2\pi n_x/L_x, 2\pi n_y/L_y)$ is the horizontal wave vector.

Substituting into (3.5)–(3.7) yields linear differential equations for $\hat{\theta}_{\mathbf{k}}$ and the Fourier components $(\hat{u}_{\mathbf{k}}, \hat{v}_{\mathbf{k}}, \hat{w}_{\mathbf{k}})$ of the velocity field $\mathbf{v}$. However, following [13] we observe that this three-dimensional problem can be reduced to a two-dimensional one: under the change of variables from $\hat{u}_{\mathbf{k}}$ and $\hat{v}_{\mathbf{k}}$ to $\hat{u}_{\mathbf{k}}\cos\varphi + \hat{v}_{\mathbf{k}}\sin\varphi$ and $-\hat{u}_{\mathbf{k}}\sin\varphi + \hat{v}_{\mathbf{k}}\cos\varphi$, where $\tan\varphi = k_y/k_x$, the equation for (the new) $\hat{v}_{\mathbf{k}}$ decouples, and hence $\hat{v}_{\mathbf{k}}(z) = 0$ by the no-slip velocity BCs. We thus obtain the Fourier space Euler-Lagrange equations

$$\frac{1}{2}\mathrm{i}k\hat{P}_{\mathbf{k}} - \frac{1}{R_e}\left(\mathrm{D}^2 - k^2\right)\hat{u}_{\mathbf{k}} = \frac{\lambda_k}{PrR_e}\hat{u}_{\mathbf{k}}, \tag{3.14}$$

$$\frac{1}{2}\mathrm{D}\hat{P}_{\mathbf{k}} - \frac{1}{R_e}\left(\mathrm{D}^2 - k^2\right)\hat{w}_{\mathbf{k}} + \tau'\hat{\theta}_{\mathbf{k}} = \frac{\lambda_k}{PrR_e}\hat{w}_{\mathbf{k}}, \tag{3.15}$$

$$\mathrm{i}k\hat{u}_{\mathbf{k}} + \mathrm{D}\hat{w}_{\mathbf{k}} = 0, \tag{3.16}$$

$$\tau'\hat{w}_{\mathbf{k}} - \left(\mathrm{D}^2 - k^2\right)\hat{\theta}_{\mathbf{k}} = \lambda_k\,\hat{\theta}_{\mathbf{k}} \tag{3.17}$$

defined on $z \in [0,1]$, where we write $k^2 = |\mathbf{k}|^2 = k_x^2 + k_y^2$ and $\mathrm{D} = d/dz$. The boundary conditions on the Fourier coefficients follow immediately from those on $\mathbf{v}$ and θ: the no-slip condition becomes $\hat{u}_\mathbf{k} = \hat{w}_\mathbf{k} = 0$ for $z = 0$ and 1, while the thermal BCs (2.17) give $\hat{\theta}_\mathbf{k} - \eta\,\mathrm{D}\hat{\theta}_\mathbf{k} = 0$ at $z = 0$, $\hat{\theta}_\mathbf{k} + \eta\,\mathrm{D}\hat{\theta}_\mathbf{k} = 0$ at $z = 1$.

At this point we observe that the solutions of (3.14)–(3.17) depend only on the magnitude and not on the direction of the horizontal wave vector $\mathbf{k}$, that is, we need consider only the wave numbers $k = |\mathbf{k}| \geq 0$; our notation λ_k for the eigenvalue reflects this.

Since among the allowed fields $\mathbf{v}$ and θ are ones containing a single Fourier mode, the spectral constraint on $\tau(z)$ is now equivalent to requiring $\lambda_k^0[\tau; R_\mathrm{e}] \geq 0$ for each k. Letting $Ra_{c,\eta}(k)$ be the critical Rayleigh number for instability of the conduction state to perturbations at wave number k, we have that $\lambda_k^0[\tau_c; R_\mathrm{e}] \geq 0$ for $R_\mathrm{e} \leq Ra_{c,\eta}(k)$, so that (for $R_\mathrm{e} > Ra_{c,\eta} = \min_k Ra_{c,\eta}(k)$) the admissibility condition on τ only needs to be checked for the finite range of wave numbers k for which $R_\mathrm{e} > Ra_{c,\eta}(k)$.

3.3 A stronger admissibility condition

The analytical solution of the Euler-Lagrange equations (3.14)–(3.17) and derivation of the optimal background τ_opt seems out of reach, even within the restricted class of piecewise linear backgrounds discussed in Section 4. Instead, one may find conditions on τ ensuring $\mathcal{Q}'_{\tau,R_\mathrm{e}} \geq 0$, and hence derive analytical bounds on Nu, via direct estimates on the quadratic form $\mathcal{Q}'_{\tau,R_\mathrm{e}}[\mathbf{v},\theta]$.

For thermal BCs other than the usual Dirichlet conditions, one does not have direct control of θ near the boundaries, and it is difficult to see how the BCs (2.17) may be used to strengthen estimates on the quadratic form, or how to utilize the explicit boundary term in $\mathcal{Q}'_{\tau,R_\mathrm{e}}$ (2.29). As demonstrated in [25] in the fixed flux (Neumann) case, though, by utilizing incompressibility and the no-slip condition on the velocity, it is possible to derive bounds while neglecting the BCs on θ.

This suggests that we introduce a stronger condition on background fields, using only the quadratic form $\mathcal{Q}_{\tau,R_\mathrm{e}}$ (2.26): we say that $\tau(z)$, satisfying the appropriate thermal BCs (2.5), is *strongly admissible* if $\mathcal{Q}_{\tau,R_\mathrm{e}}[\mathbf{v},\theta] \geq 0$ for all sufficiently smooth, horizontally periodic fields $\mathbf{v}$ and θ for which $\boldsymbol{\nabla}\cdot\mathbf{v} = 0$ and $\mathbf{v} = \mathbf{0}$ at $z = 0, 1$, where we do not specify BCs on θ. Since (by (2.29) and (2.31)) the additional boundary term which appears for $0 < \eta < \infty$ is stabilizing,

$$\begin{aligned}\mathcal{Q}'_{\tau,R_\mathrm{e}}[\mathbf{v},\theta] &= \mathcal{Q}_{\tau,R_\mathrm{e}}[\mathbf{v},\theta] + A\eta\left\langle\left(\overline{\theta_z^2}|_{z=0} + \overline{\theta_z^2}|_{z=1}\right)\right\rangle \\ &\geq \mathcal{Q}_{\tau,R_\mathrm{e}}[\mathbf{v},\theta],\end{aligned} \tag{3.18}$$

strong admissibility implies admissibility.

3.3.1 Fourier space formulation and elementary estimates

As in [25,35], using the decomposition (3.13) and incompressibility, we may write in Fourier space:

$$\mathcal{Q}_{\tau,R_\mathrm{e}}[\mathbf{v},\theta] = \int_f \left[\frac{1}{R_\mathrm{e}}|\boldsymbol{\nabla}\mathbf{v}|^2 + 2\tau' w\theta + |\boldsymbol{\nabla}\theta|^2\right] \geq A\sum_\mathbf{k}\mathcal{Q}_\mathbf{k}, \tag{3.19}$$

where $\mathcal{Q}_\mathbf{k} \equiv \mathcal{Q}_{\mathbf{k};\tau,R_\mathrm{e}}[\hat{w}_\mathbf{k},\hat{\theta}_\mathbf{k}]$ is defined by

$$\begin{aligned}\mathcal{Q}_\mathbf{k} = \int_0^1 \Bigg[&\frac{1}{R_\mathrm{e}}\left(k^2|\hat{w}_\mathbf{k}|^2 + 2|\mathrm{D}\hat{w}_\mathbf{k}|^2 + \frac{1}{k^2}|\mathrm{D}^2\hat{w}_\mathbf{k}|^2\right) \\ &+2\tau'\mathrm{Re}[\hat{w}_\mathbf{k}\hat{\theta}_\mathbf{k}^*] + \left(k^2|\hat{\theta}_\mathbf{k}|^2 + |\mathrm{D}\hat{\theta}_\mathbf{k}|^2\right)\Bigg]\,dz.\end{aligned} \tag{3.20}$$

Here (via no-slip BCs and incompressibility) $\hat{w}_\mathbf{k} = \mathrm{D}\hat{w}_\mathbf{k} = 0$ at $z = 0, 1$, while no conditions are imposed on the $\hat{\theta}_\mathbf{k}$. It follows from (3.19) that $\tau(z)$ is strongly admissible, for a given R_e, if and only if $\mathcal{Q}_\mathbf{k}[\hat{w}_\mathbf{k},\hat{\theta}_\mathbf{k}] \geq 0$ for each $\mathbf{k}$.

For future reference, following [25] we remark that the BCs on $\hat{w}_\mathbf{k}$ allow one to control the indefinite term in $\mathcal{Q}_\mathbf{k}$ near the boundary. Specifically, for $0 \leq z \leq 1/2$, using the Cauchy-Schwarz and Young's inequalities, one finds

$$\begin{aligned}|\hat{w}_\mathbf{k}(z)\,\hat{\theta}_\mathbf{k}^*(z)| \leq &\frac{z}{2\sqrt{2}}\Bigg[a_1\|\mathrm{D}\hat{w}_\mathbf{k}\|^2_{[0,\frac{1}{2}]} + \frac{1}{a_1}\|\mathrm{D}\hat{\theta}_\mathbf{k}\|^2_{[0,\frac{1}{2}]} \\ &+ \frac{a_2}{k^2}\|\mathrm{D}^2\hat{w}_\mathbf{k}\|^2_{[0,\frac{1}{2}]} + \frac{k^2}{a_2}\|\hat{\theta}_\mathbf{k}\|^2_{[0,\frac{1}{2}]}\Bigg]\end{aligned} \tag{3.21}$$

for constants a_1, $a_2 > 0$, and similarly for $1/2 \leq z \leq 1$.

4 Piecewise linear background profiles

Instead of attempting the difficult task of solving the full optimization problem for general backgrounds $\tau(z)$, we now specialize to a family of piecewise linear test functions $\tau_\delta(z)$, parametrized by $0 < \delta \leq 1/2$, which are nonconstant only over "boundary layers" of thickness δ. Since then the τ'_δ appearing in the quadratic form $\mathcal{Q}_{\tau,R_\mathrm{e}}[\mathbf{v},\theta]$, and in the corresponding Euler-Lagrange equations for the minimizing fields (3.5)–(3.7), is piecewise constant, results are much more accessible than for general $\tau(z)$.

We thus define

$$\tau(z) = \tau_\delta(z) = \begin{cases} 1/2 - \gamma(z-\delta), & 0 \leq z \leq \delta, \\ 1/2, & \delta < z < 1-\delta, \\ 1/2 - \gamma(z-(1-\delta)), & 1-\delta \leq z \leq 1, \end{cases} \tag{4.1}$$

substituting, we find the values of $\gamma = -\tau'_\delta(0) = -\tau'_\delta(1)$ and $\Delta\tau = \tau_\delta(0) - \tau_\delta(1)$, depending on δ and η, for which $\tau_\delta(z)$ satisfies the fixed Biot number thermal BCs (2.5) [35]:

$$\gamma = \frac{1+2\eta}{2(\delta+\eta)}, \qquad \Delta\tau = 2\delta\gamma = \frac{\delta(1+2\eta)}{\delta+\eta}. \tag{4.2}$$

We also compute $\int_0^1 \tau_\delta'^2\,dz = 2\delta\gamma^2 = \gamma\Delta\tau$; substituting into (3.1)–(3.2) and simplifying, we readily obtain formulas for the conservative bounds on β and ΔT for fixed Biot

number convection:

$$\beta \le \mathcal{B}_{\mathrm{pwl},\eta}(\delta, b) \equiv \mathcal{B}_\eta[\tau_\delta; b] = 1 + b\,(\gamma - 1), \tag{4.3}$$

$$\Delta T \ge \mathcal{D}_{\mathrm{pwl},\eta}(\delta, b) \equiv \mathcal{D}_\eta[\tau_\delta; b] = 1 + b\,(\Delta\tau - 1), \tag{4.4}$$

the corresponding upper bound on the Nusselt number is $Nu \le \mathcal{N}_{\mathrm{pwl},\eta}(\delta, b) \equiv \mathcal{N}_\eta[\tau_\delta; b] = \mathcal{B}_{\mathrm{pwl},\eta}(\delta, b)/\mathcal{D}_{\mathrm{pwl},\eta}(\delta, b)$. We observe that $\delta = 1/2$ gives the conduction state $\tau_c(z)$, for which $\beta = \Delta T = 1$, while for $0 < \delta \le 1/2$ we have $\gamma \ge 1$, $\Delta\tau \le 1$.

Since from (4.2) γ decreases with δ, for fixed b we obtain better upper bounds on β, and hence on Nu, by choosing δ as large as possible, subject however to the spectral constraint that τ_δ should be admissible for a given R_e.

4.1 Analytical admissibility criterion

As outlined in [35] following numerous earlier works, we may obtain explicit, though presumably weakened, analytical bounds on Nu using elementary estimates, uniform in k, directly on the Fourier space quadratic forms $\mathcal{Q}_\mathbf{k}$. We shall discuss these bounds in sufficient detail to permit comparison with the numerically obtained optimal bounds for piecewise linear backgrounds $\tau_\delta(z)$.

Using $\tau_\delta' = -\gamma$ for $z \in [0, \delta)$ and $z \in (1-\delta, 1]$, and $\tau_\delta' = 0$ elsewhere, using (3.21) we estimate the indefinite term in $\mathcal{Q}_\mathbf{k}$ as

$$\begin{aligned}\int_0^{1/2} 2\tau_\delta' \mathrm{Re}[\hat{w}_\mathbf{k}\hat{\theta}_\mathbf{k}^*]\,dz &\ge -2\gamma \int_0^\delta |\hat{w}_\mathbf{k}\hat{\theta}_\mathbf{k}^*|\,dz \\ &\ge -\frac{\gamma\delta^2}{2\sqrt{2}}\left[a_1 \|\mathrm{D}\hat{w}_\mathbf{k}\|^2_{[0,\frac{1}{2}]}\right. \\ &\quad + \frac{1}{a_1}\|\mathrm{D}\hat{\theta}_\mathbf{k}\|^2_{[0,\frac{1}{2}]} \\ &\quad \left. + \frac{a_2}{k^2}\|\mathrm{D}^2\hat{w}_\mathbf{k}\|^2_{[0,\frac{1}{2}]} + \frac{k^2}{a_2}\|\hat{\theta}_\mathbf{k}\|^2_{[0,\frac{1}{2}]}\right],\end{aligned} \tag{4.5}$$

and similarly over $z \in [1/2, 1]$. Substituting into (3.20), this gives

$$\begin{aligned}\mathcal{Q}_\mathbf{k} \ge{}& \left(\frac{2}{R_\mathrm{e}} - \frac{\gamma\delta^2\,a_1}{2\sqrt{2}}\right)\|\mathrm{D}\hat{w}_\mathbf{k}\|^2 \\ &+ \left(\frac{1}{R_\mathrm{e}} - \frac{\gamma\delta^2\,a_2}{2\sqrt{2}}\right)\frac{1}{k^2}\|\mathrm{D}^2\hat{w}_\mathbf{k}\|^2 + \frac{1}{R_\mathrm{e}}k^2\|\hat{w}_\mathbf{k}\|^2 \\ &+ \left(1 - \frac{\gamma\delta^2}{2\sqrt{2}\,a_2}\right)k^2\|\hat{\theta}_\mathbf{k}\|^2 + \left(1 - \frac{\gamma\delta^2}{2\sqrt{2}\,a_1}\right)\|\mathrm{D}\hat{\theta}_\mathbf{k}\|^2,\end{aligned} \tag{4.6}$$

where norms are over $[0, 1]$ unless otherwise specified.

We can ensure that all coefficients in (4.6) are separately nonnegative, independent of k, by letting $a_1 = a_2 = \gamma\delta^2/2\sqrt{2}$, and then choosing $\gamma^2\delta^4/8 \le 1/R_\mathrm{e}$. Recalling that $\gamma = \gamma(\delta)$ by (4.2), for fixed η and R_e this is a sufficient condition on δ for the strong admissibility of τ_δ. Define the critical value δ_a obtained by this analysis by

$$\gamma(\delta_a)^2\delta_a^4 = \frac{(1+2\eta)^2}{4(\delta_a+\eta)^2}\delta_a^4 = \frac{8}{R_\mathrm{e}} = 8\frac{b-1}{bR}, \tag{4.7}$$

then the spectral constraint on the piecewise linear profile τ_δ is certainly satisfied for $\delta \le \delta_a$, and the best bound in this approach is obtained with the choice $\delta = \delta_a$.

4.2 The optimal solution for piecewise linear backgrounds

For the piecewise linear backgrounds $\tau_\delta(z)$ defined in (4.1), the Fourier-space Euler-Lagrange equations for the minimizing fields (3.14)–(3.17) are constant coefficient, and for each k may thus be solved exactly, separately in the intervals $z \in [0, \delta)$, $(\delta, 1-\delta)$ and $(1-\delta, 1]$. This permits the complete (numerical) solution of the optimal bounding problem within the one-parameter family of background profiles $\tau = \tau_\delta$; since the optimization is over a restricted subset of all admissible backgrounds τ, it is denoted a "semi-optimal" bound for the full problem.

4.2.1 Optimization procedure

We outline the procedure for optimizing over piecewise linear backgrounds of the form $\tau_\delta(z)$; analogous discussions for related problems are presented in [16,18,23].

For each effective control parameter $R_\mathrm{e} > Ra_{c,\eta}$, we wish first to find values of δ for which τ_δ is admissible, $\mathcal{Q}'_{\tau_\delta, R_\mathrm{e}} \ge 0$ (the existence of such δ was shown by the analysis of Sect. 4.1, which demonstrated that $\delta \le \delta_a$ is sufficient), and then among these choose the largest.

Considering the horizontal wave numbers k separately, we thus let $\delta_k = \delta_k(R_\mathrm{e})$ be the largest $\delta \le 1/2$ for which the lowest eigenvalue λ_k of (3.14)–(3.17) is nonnegative, $\lambda_k^0(\delta_k, R_\mathrm{e}) \equiv \lambda_k^0[\tau_{\delta_k}; R_\mathrm{e}] \ge 0$. Observe that we certainly have $\delta_k \ge \delta_a$ for δ_a defined in (4.7); and that if $\lambda_k^0(\delta_k, R_\mathrm{e})$ is nonnegative, then so is $\lambda_k^0(\delta, R_\mathrm{e})$ for $\delta \le \delta_k$. If k is such that $R_\mathrm{e} \le Ra_{c,\eta}(k)$, then the conduction state τ_c is stable and we can set $\delta_k(R_\mathrm{e}) = 1/2$; otherwise, within the finite band of k values for which $R_\mathrm{e} > Ra_{c,\eta}(k)$, we compute δ_k as the *smallest* δ for which $\lambda_k(\delta, R_\mathrm{e}) = 0$ (if $\lambda_k(\delta, R_\mathrm{e}) = 0$ for more than one $\delta < 1/2$, then the zeros for $\delta > \delta_k$ correspond to vanishing higher eigenvalues of (3.14)–(3.17)).

We now define $\delta_c = \delta_c(R_\mathrm{e})$ as the minimum (over k) of all $\delta_k(R_\mathrm{e})$, and let $k_c = k_c(R_\mathrm{e})$ be a wave number k at which the minimum is attained (there is no additional difficulty if there is more than one such k, although this is not observed in our computations). It follows that $\lambda_k^0(\delta_c, R_\mathrm{e}) \ge 0$ for all k, so that the piecewise linear background $\tau_\delta(z)$ satisfies the spectral constraint for all Fourier modes for all $\delta \le \delta_c$, while it fails to do so for mode k_c when $\delta > \delta_c$.

For a given $R_\mathrm{e} = bR/(b-1)$, the choice $\delta = \delta_c$ thus gives the best bound using piecewise linear backgrounds

τ_δ. The corresponding upper bound on β (for $\eta < \infty$) is obtained by substituting into (4.3), to give

$$\beta \le \mathcal{B}'_{\mathrm{pwl},\eta}(b,R) \equiv \mathcal{B}_{\mathrm{pwl},\eta}(\delta_c,b) = 1 + \frac{b}{2}\frac{1-2\delta_c}{\delta_c+\eta}, \quad (4.8)$$

which depends implicitly on R, and both explicitly and implicitly on b, due to the definition of $\delta_c(R_\mathrm{e})$ by the admissibility constraint. The corresponding lower bound on ΔT (for $\eta > 0$) may be found similarly from (4.4) as

$$\Delta T \ge \mathcal{D}'_{\mathrm{pwl},\eta}(b,R) \equiv \mathcal{D}_{\mathrm{pwl},\eta}(\delta_c,b) = 1 - b\eta\frac{1-2\delta_c}{\delta_c+\eta}, \quad (4.9)$$

hence we obtain the upper bound on Nu for given R and b, $\mathcal{N}'_{\mathrm{pwl},\eta}(b,R) = \mathcal{B}'_{\mathrm{pwl},\eta}(b,R)/\mathcal{D}'_{\mathrm{pwl},\eta}(b,R)$.

For given Biot number η and control parameter R, the best bounds available for piecewise linear backgrounds $\tau_\delta(z)$ may now be obtained by optimizing over the balance parameter $b > 1$. For $\eta < \infty$, we denote the semi-optimal conservative upper bound on β by

$$\beta \le \widetilde{\mathcal{B}}_\eta(R) \equiv \min_{b>1} \mathcal{B}'_{\mathrm{pwl},\eta}(b,R), \quad (4.10)$$

where the minimum is attained at $b = b_{c,\eta}(R) > 1$; for simplicity we have dropped "pwl" from our notation, but it remains understood that we optimize only over piecewise linear background profiles. Substituting $b = b_{c,\eta}$ allows us to deduce the semi-optimal values of R_e, and hence of δ_c and k_c, as functions of R for a given η.

For $0 < \eta < \infty$ we may now compute the corresponding lower bound on ΔT by $\widetilde{\mathcal{D}}_\eta(R) \equiv \mathcal{D}'_{\mathrm{pwl},\eta}(b_{c,\eta},R)$ (in the fixed flux case $\eta = \infty$, for which $\beta = \widetilde{\mathcal{B}}_\eta(R) = 1$, we maximize $\mathcal{D}'_{\mathrm{pwl},\eta}(b,R)$ over b directly). Finally, we obtain the semi-optimal upper bound on the Nusselt number (as a function of R and η):

$$Nu \le \widetilde{\mathcal{N}}_\eta(R) \equiv \widetilde{\mathcal{B}}_\eta(R)/\widetilde{\mathcal{D}}_\eta(R). \quad (4.11)$$

(We remark that in optimizing over b, for $0 < \eta < \infty$ we minimize $\mathcal{B}'_{\mathrm{pwl},\eta}(b,R)$ as in (4.10), rather than directly working with the Nusselt number bound $\mathcal{N}'_{\mathrm{pwl},\eta}(b,R)$. This is because for some $b > 1$, the lower bound $\mathcal{D}'_{\mathrm{pwl},\eta}(b,R)$ on ΔT from (4.9) can become negative – though it is positive at $b = b_{c,\eta}(R)$ – which causes difficulties for minimizing $\mathcal{N}'_{\mathrm{pwl},\eta}(b,R)$.)

The computation culminating in (4.11) provides (for given η) an upper bound on the Nusselt number Nu as a function of the control parameter R, which measures the strength of thermal driving through the applied boundary conditions. Typically, though, one seeks the relationship between Nu and the Rayleigh number Ra, a measure of the averaged temperature drop across the fluid, which for $R > Ra_{c,\eta}$ only coincides with R in the fixed temperature case $\eta = 0$. Thus in general we also need to estimate Ra, which is done through the lower bound on ΔT using (2.12); we obtain

$$Ra = R\,\Delta T \ge R\,\widetilde{\mathcal{D}}_\eta(R) \equiv \widetilde{\mathcal{R}}_\eta(R). \quad (4.12)$$

Since both $\widetilde{\mathcal{R}}_\eta(R)$ and $\widetilde{\mathcal{N}}_\eta(R)$ are increasing in R, we can now bound R, and hence Nu, from above in terms of Ra. In principle, this involves inverting the relationship (4.12), to yield $Nu \le \widetilde{\mathcal{N}}_\eta(\widetilde{\mathcal{R}}_\eta^{-1}(Ra)) \equiv Nu_{\mathrm{bound},\eta}(Ra)$. In practice, we plot the bounds found in (4.11) and (4.12), parametrized by R, and hence extract the scaling of the Nu–Ra bounding relationship.

4.2.2 Solution of Euler-Lagrange equations

The essential first step in the above bounding and optimization procedure is the computation of $\delta_k(R_\mathrm{e})$, given by the vanishing of the lowest eigenvalue of (3.14)–(3.17), $\lambda_k^0(\delta_k, R_\mathrm{e}) = 0$. We eliminate the pressure $\hat{P}_\mathbf{k}$ from (3.14)–(3.15) by taking $[\mathrm{i}k\cdot(3.15) - \mathrm{D}(3.14)]$; setting $\lambda_k = 0$, (3.14)–(3.17) then give

$$\left(\mathrm{D}^2 - k^2\right)\left(\mathrm{D}\bar{u} + k^2 w\right) - k^2 R_\mathrm{e}\,\tau'\theta = 0, \quad (4.13)$$

$$\tau' w - \left(\mathrm{D}^2 - k^2\right)\theta = 0, \quad (4.14)$$

$$\bar{u} + \mathrm{D}w = 0, \quad (4.15)$$

where we have simplified notation by dropping hats and subscripts, and written $\bar{u} = \mathrm{i}ku$.

Equations (4.13)–(4.15) should now be solved separately in each region of definition of $\tau_\delta(z)$ from (4.1). However, one can use the $z \mapsto 1 - z$ symmetry of the problem to show that the lowest eigenfunctions for w and θ are even about $z = 1/2$ (see [18], Appendix C for a related discussion). Thus we need only to solve the problem in the two intervals $[0,\delta)$ and $(\delta,1/2]$ (denoted by Regions I and II, respectively) subject to the boundary conditions at $z = 0$, symmetry conditions at $z = 1/2$ and matching conditions at $z = \delta$.

In Region I, $\tau' = -\gamma$, and the solution to (4.13)–(4.15) in the form of complex exponentials is

$$\begin{aligned} w &= A_1 e^{p_1 z} + A_2 e^{-p_1 z} + A_3 e^{p_2 z} + A_4 e^{-p_2 z} \\ &\quad + A_5 e^{p_3 z} + A_6 e^{-p_3 z}, \\ \bar{u} &= -\left[A_1 p_1 e^{p_1 z} - A_2 p_1 e^{-p_1 z} + A_3 p_2 e^{p_2 z} - A_4 p_2 e^{-p_2 z}\right. \\ &\quad \left. + A_5 p_3 e^{p_3 z} - A_6 p_3 e^{-p_3 z}\right], \\ \theta &= \frac{\rho^2}{k^2\gamma R_\mathrm{e}}\left[e^{2\pi\mathrm{i}/3}\left(A_1 e^{p_1 z} + A_2 e^{-p_1 z}\right)\right. \\ &\quad \left. + e^{-2\pi\mathrm{i}/3}\left(A_3 e^{p_2 z} + A_4 e^{-p_2 z}\right) + \left(A_5 e^{p_3 z} + A_6 e^{-p_3 z}\right)\right], \end{aligned} \quad (4.16)$$

where $\rho = \left(k^2\gamma^2 R_\mathrm{e}\right)^{1/3}$, and $p_n = \sqrt{k^2 + \rho e^{\mathrm{i}\pi(1-2n/3)}}$ for $n = 1,2,3$.

In Region II, where $\tau' = 0$, the fields w and θ are decoupled, and the general solution in exponential form is

$$\begin{aligned} w &= B_1 e^{kz} + B_2 z e^{kz} + B_3 e^{-kz} + B_4 z e^{-kz}, \\ \bar{u} &= -\left[B_1 k e^{kz} + B_2(1+kz)e^{kz}\right. \\ &\quad \left. - B_3 k e^{-kz} + B_4(1-kz)e^{-kz}\right], \\ \theta &= B_5 e^{kz} + B_6 e^{-kz}. \end{aligned} \quad (4.17)$$

The solution (4.16)–(4.17) must satisfy the following conditions:

$$\bar{u}(0) = w(0) = 0, \tag{4.18}$$

$$\theta(0) - \eta\,\mathrm{D}\theta(0) = 0, \tag{4.19}$$

$$\bar{u}(1/2) = \mathrm{D}^2\bar{u}(1/2) = \mathrm{D}\theta(1/2) = 0, \tag{4.20}$$

$$[w]_\delta = [\mathrm{D}w]_\delta = [\mathrm{D}^2 w]_\delta = [\mathrm{D}^3 w]_\delta = [\theta]_\delta = [\mathrm{D}\theta]_\delta = 0. \tag{4.21}$$

Here (4.18) is the no-slip condition on the velocity field, while the thermal BCs (2.17) are represented by (4.19). The condition that w and θ are even, and hence $\bar{u} = -\mathrm{D}w$ is odd, about $z = 1/2$ is expressed in (4.20), where the first two equations are equivalent to $\mathrm{D}w(1/2) = \mathrm{D}^3 w(1/2) = 0$. Lastly, we require that w and its first three derivatives, and θ and its first derivative, are continuous at $z = \delta$ (which also implies the necessary continuity of $\bar{u}$); this condition, given in (4.21), matches the solution (4.16) in Region I to the Region II solution (4.17), where we have used the notation $[f]_\delta = f(\delta+) - f(\delta-)$ to indicate the jump in a function $f(z)$ across $z = \delta$.

Equations (4.18)–(4.21) give 12 linear equations in the 12 unknown constants $A_1, \ldots, A_6$, $B_1, \ldots, B_6$, which we may write in the form $\mathsf{M}_\eta \mathbf{c} = \mathbf{0}$, where $\mathbf{c} = [A_1, \ldots, B_6]^T$ is the vector of unknowns, and $\mathsf{M}_\eta = \mathsf{M}_\eta(\delta, k, R_\mathrm{e})$ is the 12×12 matrix of coefficients defined by (4.18)–(4.21) with (4.16)–(4.17). Since we require a nontrivial solution for w, $\bar{u}$ and θ, the determinant of the coefficient matrix M_η must vanish; this defines δ_k as the smallest δ for which $\det \mathsf{M}_\eta(\delta, k, R_\mathrm{e}) = 0$.

We thus compute δ_k numerically by adjusting δ to find a zero of $\det \mathsf{M}_\eta(\delta, k, R_\mathrm{e})$, being careful to ensure that it is the first zero. The remaining steps in the computation involve successive minimization procedures, and have been outlined above: we minimize δ_k over k to find δ_c, then minimize the bound $\mathcal{B}_{\mathrm{pwl},\eta}(\delta_c, b)$ over $b > 1$ to optimize the bound on Nu for a given R.

4.2.3 Notes on the implementation

We performed our computations using the double precision arithmetic of MATLAB, using the built-in routine `fminbnd` for the three separate optimizations (over δ, k and b, successively). Each computation was considerably speeded up by providing well-chosen search intervals to the minimization routines: intervals bracketing the desired minima were predicted by extrapolation from the scaling observed in calculations at smaller R, or from preliminary computations with lower tolerance.

The first step of the numerical solution procedure required the calculation of δ_k, for given k and R_e; after checking that $R_\mathrm{e} > Ra_{c,\eta}(k)$ (if false, we set $\delta_k = 1/2$), we obtained δ_k by seeking the first zero of $\det \mathsf{M}_\eta$. Since the matrix of coefficients $\mathsf{M}_\eta(\delta, k, R_\mathrm{e})$ is in general complex-valued, so is its determinant, implying that we needed to find simultaneous zeros of the real and imaginary parts. In our experience, though, the real part of $\det \mathsf{M}_\eta(\delta, k, R_\mathrm{e})$ vanished for all δ near $\delta_k(R_\mathrm{e})$ (up to small numerical error); we thus located an interval containing δ_k by sweeping through δ looking for a sign change of $\mathrm{Im}[\det \mathsf{M}_\eta(\delta, k, R_\mathrm{e})]$, and then computed δ_k more accurately by minimizing $|\det \mathsf{M}_\eta(\delta, k, R_\mathrm{e})|$ using `fminbnd`.

Numerical challenges in this computation arose from the properties of the coefficient matrix $\mathsf{M}_\eta(\delta, k, R_\mathrm{e})$, and the finely balanced cancellations that permit its determinant to vanish. Due to the growth of terms such as $e^{k/2}$ and $ke^{k/2}$ (from (4.20)), beyond an η-dependent maximum value of R_e – ranging from about $R_\mathrm{e} \approx 10^8$ for $\eta = 0$ to $R_\mathrm{e} \approx 10^{13}$ for $\eta = \infty$ – without rescaling the calculations were subject to numerical overflow. Using the observed scaling of δ_c and k_c with R_e, though, by suitable row and column operations on M_η the leading R_e-dependent terms were scaled out (see [38] for more details). This enabled us to continue the computations to much higher R_e values (for all η, the corresponding bounds on Ra from (4.12) extended beyond 10^{30}), sufficient to identify the asymptotic scaling in all our cases, before the loss of precision due to cancellation of almost equal terms became insurmountable in double precision (see [16] for a similar discussion for the numerically more subtle infinite Prandtl number convection, where it was found necessary to go to multiple precision arithmetic to extract the asymptotic scaling).

As a check on the accuracy of our computations, we recovered the eigenfunctions for $\delta = \delta_c(R_\mathrm{e})$ and $k = k_c(R_\mathrm{e})$, checking for smoothness at $z = \delta_c$ (4.21) and satisfaction of the boundary and symmetry conditions (4.18)–(4.20). We found that for all η, the eigenfunctions remained smooth up to at least $R_\mathrm{e} \approx 10^{24}$. For higher R_e, there was some loss of smoothness at $z = \delta_c$ through numerical error; however, in our experience the computed bounds such as (4.11) and (4.12) remained smoothly dependent on R well beyond any breakdown of the eigenfunctions.

We remark that while in (4.16)–(4.17) we wrote down the solution to (4.13)–(4.15) in the form of exponential functions, we could equally well have expressed w, $\bar{u}$ and θ using hyperbolic functions. Indeed, by the symmetry conditions (4.20) three coefficients would then immediately vanish, leaving us to find zeros of the determinant of only a 9×9 matrix. We found (see [38]) that the exponential and hyperbolic forms of the coefficient matrix, after suitable rescaling, permitted computation to equally high values of R and yielded the same numerical bounds. However, while the hyperbolic matrix (unsurprisingly) better enforced the symmetry at $z = 1/2$, the exponential matrix appeared to yield more accurate eigenfunctions within the boundary layer and near $z = \delta_c$. Consequently we have largely used the exponential form of the coefficient matrix, obtained from (4.16)–(4.17) with (4.18)–(4.21), for our computations of the semi-optimal bound.

5 Analytical and numerical conservative bounds

In this section we present and compare the conservative analytical and numerical bounds on convective heat

transport, optimized over the restricted class of one-parameter piecewise linear backgrounds of the form $\tau_\delta(z)$ (4.1). We first discuss the limiting fixed temperature and fixed flux cases, as these demonstrate the two distinct scaling regimes and provide a reference for general Biot number η.

5.1 Fixed temperature boundary conditions

5.1.1 Analytical estimates

For fixed temperature (Dirichlet) thermal BCs ($\eta = 0$), we have $\Delta T = \Delta\tau = 1$, and by (4.2) $\gamma = 1/2\delta$. The sufficient analytical condition (4.7) for strong admissibility of $\tau_\delta(z)$ is then $\delta \le \delta_a$ where

$$\delta_a^2 = \frac{32}{R_e} = 32\frac{b-1}{bR}. \tag{5.1}$$

Hence the bound (4.3) becomes

$$Nu = \beta \le \mathcal{B}_{\mathrm{pwl},0}(\delta_a, b) = 1 - b + \frac{1}{8\sqrt{2}}\frac{b^{3/2}}{(b-1)^{1/2}}R^{1/2}. \tag{5.2}$$

Optimizing this bound by minimizing $b^{3/2}(b-1)^{-1/2}$ over $b > 1$, we find that the optimal choice of the balance parameter is $b_{a,0} = 3/2$, in which case $R_e = 3R$ and $\delta_a = 4\sqrt{2/3}\,R^{-1/2}$ from (5.1). Setting $b = 3/2$ in (5.2) then gives the best analytical ("a") bound on Nu available in this approach, $\mathcal{B}_{\mathrm{pwl},0}(\delta_a, b_{a,0}) = -1/2 + (3/4)\delta_a^{-1}$, which we denote by $\widetilde{\mathcal{N}}_{a,0}(R) = \widetilde{\mathcal{B}}_{a,0}(R)$. Recalling that for fixed temperature BCs, the control parameter R is just the Rayleigh number Ra, this rigorously bounds the Nusselt number for fixed temperature BCs (valid for all $R = Ra$ sufficiently large that $\delta_a \le 1/2$) by

$$Nu \le \widetilde{\mathcal{N}}_{a,0} = -\frac{1}{2} + \frac{3\sqrt{6}}{32}Ra^{1/2} \approx -\frac{1}{2} + 0.230\,Ra^{1/2}. \tag{5.3}$$

We note that our bound is slightly better than the initial rigorous bound $Nu \le \frac{1}{4}Ra^{1/2} - 1$ derived by Doering and Constantin [13] using a piecewise linear background, which did not make use of a balance parameter [24], although slightly worse than their improved analytical bound $Nu \le \frac{1}{6}Ra^{1/2} - 1$ obtained by strengthening the spectral constraint, and finding the optimal solution of the resulting simplified variational problem [13].

5.1.2 Semi-optimal bounds

The *Nu-Ra* scaling found by solving the semi-optimal bounding problem numerically, as described in Section 4.2, is shown in Figure 1. The inset confirms that the bound bifurcates at the well-known critical Rayleigh number for fixed temperature convection, $Ra_{c,0} \approx 1707.76$ [39], as expected from the discussion in Section 3.1.1. However, the bound bifurcates discontinuously from $Nu = 1$ for Ra just above $Ra_{c,0}$, as also seen in [23], since we have constrained

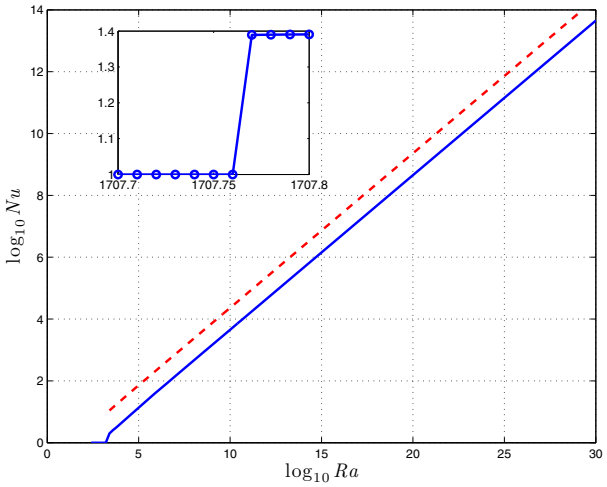

Fig. 1. (Color online) Fixed temperature BCs: dependence of the conservative numerical upper bound $\widetilde{\mathcal{N}}_0$ on the Nusselt number Nu (solid line), on the Rayleigh number Ra (which here equals the control parameter R); we find $\widetilde{\mathcal{N}}_0 \sim 0.045038 Ra^{0.5}$, where for $Ra \gtrsim 10^{25}$ the computed exponent is 0.5 with an error of less than 10^{-12}; the dashed line shows the analytical bound (5.3), $\widetilde{\mathcal{N}}_{a,0} = -1/2 + (3\sqrt{6}/32)Ra^{1/2}$. Inset: behaviour of the bound near the bifurcation value $Ra_{c,0} \approx 1707.76$.

the slope of our backgrounds $\tau_\delta(z)$ to vanish in the middle, which does not accurately capture the critical mode at bifurcation; a negative slope in the bulk would presumably permit a smoother transition in the bound [16].

Our overall numerical bound, optimized over piecewise linear backgrounds $\tau_\delta(z)$, scales as $Nu \lesssim 0.04504\,Ra^{1/2}$. The prefactor significantly improves the analytical bound (5.3), and is within less than a factor of two of the optimal bound for fixed temperature, arbitrary Prandtl number convection, $Nu - 1 \le 0.02634\,Ra^{1/2}$, obtained by Plasting and Kerswell [19]; it is also weaker than the bound $Nu - 1 \le 0.0335\,Ra^{1/2}$ obtained by optimizing over piecewise quadratic profiles [15,40].

The intermediate quantities in this bounding calculation all scale as predicted by the analysis; see [38]. In particular, the balance parameter b_c approaches 1.5 (see Fig. 7 below), with $b_c - 1.5 \sim 17\,Ra^{-1/2}$, so that $R_e \to 3Ra$. With $\widetilde{\mathcal{N}}_0 \sim b_c/2\delta_c \sim 3/4\delta_c$, we find also that $\delta_c \sim 16.65\,Ra^{-1/2}$ at the Fourier mode $k_c \sim 0.07215\,Ra^{1/2}$, so $\delta_c k_c \sim 1.2015$ (see Fig. 6a); recall that k_c is not available from the analysis uniform in wave number.

5.2 Fixed flux boundary conditions

5.2.1 Analytical estimates

We review the case of fixed flux (Neumann) boundaries ($\eta = \infty$) originally discussed in [25], for which the thermal BCs imply $\beta = \gamma = 1$, $\Delta\tau = 2\delta$ by (4.2), the spectral constraint is satisfied for $\delta \le \delta_a$ given by (4.7), and

using (4.4) we have the lower bound on the averaged temperature drop $\Delta T \geq \mathcal{D}_{\mathrm{pwl},\infty}(\delta, b) = 1 - b + 2\delta\, b$.

Since $b > 1$, in order for $\mathcal{D}_{\mathrm{pwl},\infty}$ to remain positive as $R \to \infty$ (so $\delta \to 0$), we need $b - 1 = \mathcal{O}(\delta)$, which suggests the Ansatz $b = 1 + c\,\delta$ for some $\mathcal{O}(1)$ constant $c > 0$. This implies $R_{\mathrm{e}} = (1 + c\,\delta)R/c\,\delta \sim R/c\,\delta$ asymptotically for large R (small δ), so that (4.7) becomes

$$\delta_a^4 = 8\, R_{\mathrm{e}}^{-1} \sim 8c\,\delta_a\, R^{-1}, \tag{5.4}$$

and hence $\delta_a \sim 2c^{1/3}R^{-1/3}$ and $R_{\mathrm{e}} \sim 2^{-1}(R/c)^{4/3}$. Substituting for b and $\delta = \delta_a$ in (4.4), we find

$$\begin{aligned} Nu^{-1} = \Delta T &\geq \mathcal{D}_{\mathrm{pwl},\infty}(\delta_a, 1 + c\,\delta_a) \\ &= (2 - c)\,\delta_a + 2c\,\delta_a^2 \\ &\sim (2 - c)\,\delta_a \sim 2c^{1/3}(2 - c)\,R^{-1/3}. \end{aligned} \tag{5.5}$$

The maximum value of $2c^{1/3}(2 - c)$ is $3 \cdot 2^{-1/3}$ when $c = c_{a,\infty} = 1/2$. We conclude that $\widetilde{\mathcal{D}}_{a,\infty}(R) = \mathcal{D}_{\mathrm{pwl},\infty}(\delta_a, 1 + \delta_a/2) \sim 3\,\delta_a/2 \sim 3\,(2R)^{-1/3}$ is the best lower bound on ΔT in this approach, giving the R-dependent asymptotic upper bound on Nu

$$Nu \leq \widetilde{\mathcal{N}}_{a,\infty}(R) = \left[\widetilde{\mathcal{D}}_{a,\infty}(R)\right]^{-1} \sim 3^{-1}2^{1/3}R^{1/3}. \tag{5.6}$$

In order to find the dependence of Nu on the Rayleigh number Ra, we bound $Ra = R\Delta T$ (2.12) from below,

$$Ra \geq \widetilde{\mathcal{R}}_{a,\infty}(R) = R\,\widetilde{\mathcal{D}}_{a,\infty}(R) \sim 3 \times 2^{-1/3}R^{2/3}. \tag{5.7}$$

Finally, we can rewrite (5.6)–(5.7) to estimate the Nusselt number Nu in terms of the effective control parameter R_{e}, the control parameter R and the Rayleigh number Ra, as in [25]:

$$Nu \leq \widetilde{\mathcal{N}}_{a,\infty} \sim \frac{2^{1/4}}{3}R_{\mathrm{e}}^{1/4} \sim \frac{2^{1/3}}{3}R^{1/3} \tag{5.8}$$

$$\lesssim \sqrt{\frac{2}{27}}Ra^{1/2} \approx 0.272\, Ra^{1/2}. \tag{5.9}$$

5.2.2 Semi-optimal bounds

We show the numerically obtained Nu–Ra bounds in Figure 2; the result is $Nu \lesssim 0.07808\, Ra^{1/2}$. This optimal bound over piecewise linear profiles $\tau_\delta(z)$ improves on the previous analytical bound (5.9) $Nu \leq 0.272\, Ra^{1/2}$ [25]. Again, the bound bifurcates, discontinuously, at the critical Rayleigh number for fixed flux convection, $Ra_{c,\infty} = 6! = 720$ [37,41]. The overall bound is arrived at via the intermediate scalings $Nu = (\Delta T)^{-1} \lesssim 0.21\, R_{\mathrm{e}}^{1/4}$ and $Nu \lesssim 0.1827\, R^{1/3}$, consistent with (5.8). The decay of the optimal numerically computed balance parameter b_c to 1 satisfies $b_c - 1 \sim c_\infty\delta_c$ for $c_\infty = 0.5$, as predicted analytically. In the large-R limit, the numerical bound is consistent with the prediction $\widetilde{\mathcal{N}}_\infty\delta_c \sim 2/3$ (compare with $\widetilde{\mathcal{N}}_0\delta_c \sim 3/4$ in the fixed temperature case); where δ_c and the corresponding k_c are related via $\delta_c k_c \sim 0.6161$, which is about half of the corresponding fixed temperature value (see Fig. 6a below).

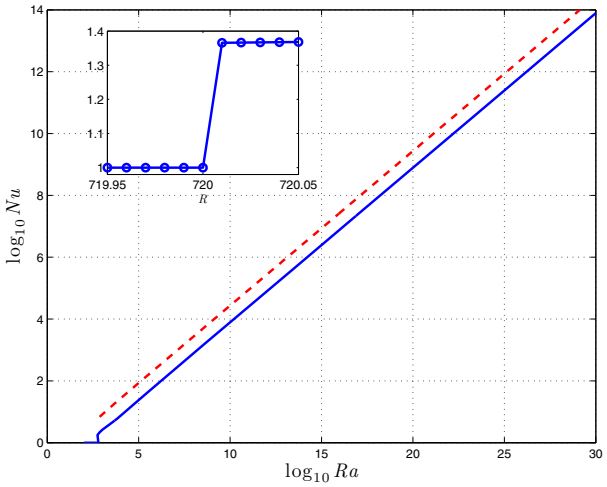

Fig. 2. (Color online) Fixed flux BCs: the conservative numerical upper bound $\widetilde{\mathcal{N}}_\infty = \widetilde{\mathcal{D}}_\infty^{-1}$ on the Nusselt number Nu (solid line), plotted against the (numerical) lower bound $\widetilde{\mathcal{R}}_\infty = R\widetilde{\mathcal{D}}_\infty$ on the Rayleigh number Ra; we compute $\widetilde{\mathcal{N}}_\infty \sim 0.07808\widetilde{\mathcal{R}}_\infty^{0.5}$, where the numerical exponent is about $0.5 + 10^{-5}$; the dashed line shows the analytical bound (5.3), $\widetilde{\mathcal{N}}_{a,\infty} \leq \sqrt{2/27}\,\widetilde{\mathcal{R}}_{a,\infty}^{1/2}$. Inset: Behaviour of the bound near the bifurcation value $Ra_{c,\infty} = 720$.

5.3 Mixed boundary conditions with fixed Biot number

For general mixed (Robin) thermal BCs (2.5) with fixed Biot number η, using (4.2) in (4.7) a sufficient condition for strong admissibility of the background is $\delta \leq \delta_a$, where

$$\gamma(\delta_a)^2\delta_a^4 = \frac{(1 + 2\eta)^2}{4(\delta_a + \eta)^2}\delta_a^4 = \frac{8}{R_{\mathrm{e}}} = 8\,\frac{b - 1}{b\,R}. \tag{5.10}$$

For fixed $0 < \eta < \infty$, the scaling of δ_a with R, and hence the overall structure of the bounds, behaves either as the fixed temperature or as the fixed flux case, depending on whether δ_a is larger or smaller than η, respectively. However, since $\delta_a \to 0$ as $R \to \infty$ ($Ra \to \infty$), asymptotically for large R the bounds are as for fixed flux BCs for any $\eta > 0$.

Specifically, if $\delta_a \gg \eta$ (so necessarily $\eta \ll 1$), (4.2) implies $\gamma \sim 1/2\delta_a$, $\Delta\tau \sim 1$, and in this asymptotic limit the bounds of Section 5.1 carry over directly. More generally, whenever $\delta_a \geq \eta$ we have $\gamma \geq 1/(4\delta_a)$ and $\Delta\tau \geq 1/2$; that is, γ grows as $\mathcal{O}(\delta_a^{-1})$ while $\Delta\tau$ is bounded below away from zero. It is then straightforward to verify that quantities scale as in the fixed temperature case: for instance, $b - 1 = \mathcal{O}(1)$, $\Delta T \geq \mathcal{O}(1)$, $Ra = \mathcal{O}(R) = \mathcal{O}(R_{\mathrm{e}})$, $\delta_a = \mathcal{O}(R_{\mathrm{e}}^{-1/2}) = \mathcal{O}(Ra^{-1/2})$, and $Nu \leq \mathcal{O}(R^{1/2}) \leq \mathcal{O}(Ra^{1/2})$.

This "fixed temperature scaling regime" persists with increasing R, until δ_a has decreased to $\delta_a = \eta$, which by the above scaling predictions occurs at a transition value $R = R_{\mathrm{t}}(\eta) = \mathcal{O}(\eta^{-2})$.

As R increases above $R_{\mathrm{t}}(\eta)$, we have $\delta_a \leq \eta$, and the system enters a new "fixed flux scaling regime", which is absent for fixed temperature BCs ($\eta = 0$). When $0 < \delta \leq \delta_a \leq \eta$, we find $(2 + \eta^{-1})/4 \leq \gamma < (2 + \eta^{-1})/2$ and $\delta(2 + \eta^{-1})/2 \leq \Delta\tau < \delta(2 + \eta^{-1})$, so that for fixed $\eta > 0$,

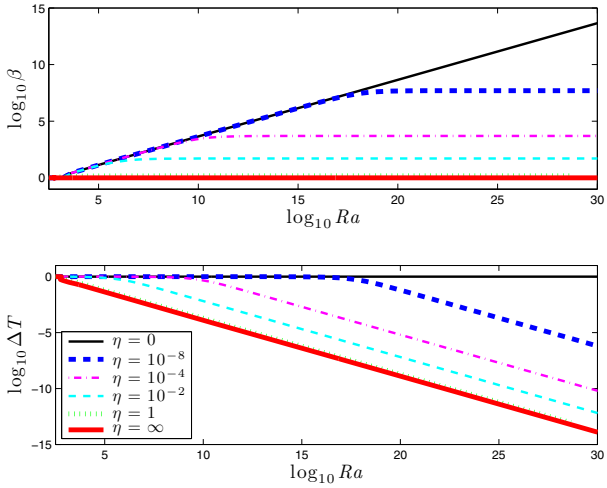

Fig. 3. (Color online) General Biot number BCs: conservative numerical upper bound $\widetilde{\mathcal{B}}_\eta$ on β (top) and lower bound $\widetilde{\mathcal{D}}_\eta$ on ΔT (bottom), as functions of the (numerical) lower bound $\widetilde{\mathcal{R}}_\eta$ on the Rayleigh number Ra, for Biot numbers $\eta = 0$ (fixed temperature: thin line), $\eta = 10^{-8}$, $\eta = 10^{-4}$, $\eta = 10^{-2}$, $\eta = 1$ (here hardly distinguishable from the fixed flux case), and $\eta = \infty$ (fixed flux: thick solid line); η is increasing from top to bottom in both figures. For $\eta = 0$, $\Delta T = 1$ and β increases without bound; while for any $\eta > 0$, β is bounded above and $\Delta T \to 0$ for large Ra. Note the distinct transition between "fixed temperature" and "fixed flux" scaling for $\eta \ll 1$.

$\Delta\tau$ decays as $\mathcal{O}(\delta)$, while γ is bounded above. By the same argument as in Section 5.2, for fixed $\eta > 0$ to ensure a positive lower bound $\mathcal{D}_{\mathrm{pwl},\eta}(\delta, b)$ on ΔT when $\delta \le \delta_a$, the balance parameter b should scale as $b - 1 = \mathcal{O}(\delta)$, which implies $\Delta T \ge \mathcal{O}(\delta)$. It follows that, for $\eta > 0$ and sufficiently large R, quantities scale as in the fixed flux case, with $\delta_a = \mathcal{O}(R_{\mathrm{e}}^{-1/4}) = \mathcal{O}(R^{-1/3})$, $Ra \ge \mathcal{O}(R^{2/3})$, and $Nu \le \mathcal{O}(R^{1/3}) \le \mathcal{O}(Ra^{1/2})$.

From the bounds, we can deduce the significant physical difference between the two scaling regimes: In the fixed temperature regime, for increasing driving as measured by the control parameter R, the Nusselt number $Nu = \beta/\Delta T$ increases due to growth in the dimensionless averaged boundary heat flux β, while ΔT decreases only slightly. For nonzero Biot number, however, β eventually saturates, and in the large-R fixed flux regime, the further growth of Nu is due to decrease in ΔT, the nondimensional averaged temperature drop across the fluid. This behaviour is clearly observed in the numerical bounds on β and ΔT shown in Figure 3.

We remark that when the boundaries are sufficiently poorly conducting that $\eta \ge 1/2$, we always have $\delta_a \le \eta$, and only the fixed flux regime is present, as is seen in Figure 3 for $\eta = 1$. A transition between distinct scaling regimes is found only in systems with highly, but imperfectly, conducting boundaries, so $0 < \eta \ll 1$; see [35] for more discussion.

5.3.1 Analytical scaling in the large-R asymptotic limit

We derive the scaling of the bounds in the strong driving limit, so that $\delta \le \delta_a \ll 1$, assuming also that we are well within the "fixed flux regime" described above; that is, $R \gg R_{\mathrm{t}}(\eta)$, so $\delta_a \ll \eta$. Since then $\Delta\tau = \mathcal{O}(\delta(2+\eta^{-1})) \ll 1$, as in the fixed flux case we need to choose the balance parameter $b > 1$ so that $b-1$ and $\Delta\tau$ are of the same order, to ensure a positive lower bound $\mathcal{D}_{\mathrm{pwl},\eta}(\delta, b)$ on ΔT. Hence we choose $b = 1 + c\,\delta$ for some $c = c(\eta)$, with $c\,\delta \ll 1$ in this asymptotic limit.

For $\delta \ll \eta$ we have $\gamma(\delta) \sim (2+\eta^{-1})/2$, and for $c\,\delta \ll 1$, $R_{\mathrm{e}} = (1 + c\,\delta)R/c\delta \sim R/c\delta$. The sufficient admissibility condition (5.10) on δ then becomes

$$\delta_a^4 \sim 32\left(2+\eta^{-1}\right)^{-2} R_{\mathrm{e}}^{-1} \sim 32c\,\delta_a\left(2+\eta^{-1}\right)^{-2} R^{-1},$$

or

$$\delta_a \sim 2^{5/3} c^{1/3}\left(2+\eta^{-1}\right)^{-2/3} R^{-1/3}. \tag{5.11}$$

Using (4.2)–(4.4), in this limit we estimate the bounds on β and ΔT as

$$\beta \le \mathcal{B}_{\mathrm{pwl},\eta}(\delta, 1+c\delta) = \frac{1 + 2\eta + c\,\delta(1-2\delta)}{2(\delta+\eta)} \sim \frac{1+2\eta}{2\eta}$$

and

$$\Delta T \ge \mathcal{D}_{\mathrm{pwl},\eta}(\delta, 1+c\delta) = \frac{\delta[1 - c\eta + 2\eta(1+c\delta)]}{\delta+\eta} \sim \frac{\delta}{\eta}\left[1 + (2-c)\eta\right], \tag{5.12}$$

and hence find an upper bound on $Nu = \beta/\Delta T$,

$$Nu \le \mathcal{N}_{\mathrm{pwl},\eta}(\delta, 1+c\delta) \sim \frac{1}{2\delta}\frac{1+2\eta}{1+(2-c)\eta} \tag{5.13}$$

for any $\delta \le \delta_a$. Substituting for δ_a from (5.11), the best asymptotic bound on Nu for a given R and $\eta > 0$ is thus

$$\mathcal{N}_{\mathrm{pwl},\eta}(\delta_a, 1+c\,\delta_a) \sim \frac{(1+2\eta)^{5/3}}{2^{8/3}\,\eta^{2/3}}\frac{R^{1/3}}{c^{1/3}\left[1+(2-c)\eta\right]}. \tag{5.14}$$

The maximum value of $c^{1/3}\left[1+(2-c)\eta\right]$ for fixed $\eta > 0$ is $3 \times 2^{-8/3}\eta^{-1/3}(1+2\eta)^{4/3}$, attained at

$$c = c_{a,\eta} = \left(2+\eta^{-1}\right)/4, \tag{5.15}$$

note that with $\delta \ll \min\{1, \eta\}$, we have $c_{a,\eta}\,\delta \ll 1$, as required. Substituting for this optimal c in (5.13), we find that the bound on Nu scales as $2/(3\delta)$ in this fixed flux regime (compare the fixed temperature analytical scaling $3/(4\delta)$). Using $c = c_{a,\eta}$ from (5.15) in (5.14), we now find that the optimal analytical R-dependent upper bound on Nu for general nonzero Biot number η in this approach is

$$Nu \le \widetilde{\mathcal{N}}_{a,\eta}(R) \sim 3^{-1}\left(2+\eta^{-1}\right)^{1/3} R^{1/3} \tag{5.16}$$

(which translates to $Nu \le 2^{-1/4}3^{-1}(2+\eta^{-1})^{1/2}R_{\mathrm{e}}^{1/4}$). That the prefactor in (5.16) diverges as $\eta \to 0$ confirms

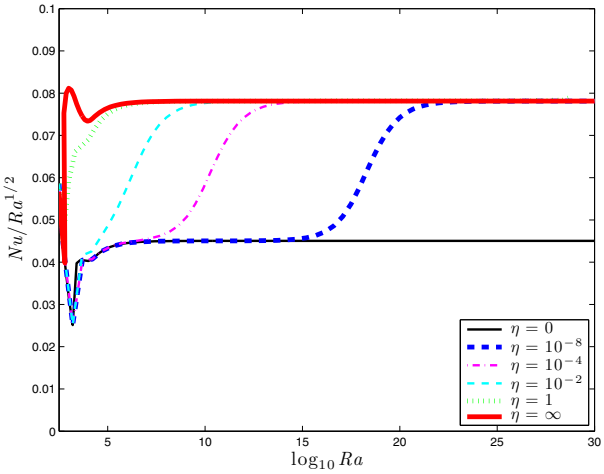

Fig. 4. (Color online) General Biot number BCs: the upper bound $\widetilde{\mathcal{N}}_\eta$ on the Nusselt number Nu, scaled by $\widetilde{\mathcal{R}}_\eta^{1/2}$, as a function of $\widetilde{\mathcal{R}}_\eta$, the lower bound on the Rayleigh number Ra. For any $\eta > 0$ the asymptotic bound coincides with that in the fixed flux case, $Nu \leq 0.078\, Ra^{1/2}$ as $Ra \to \infty$.

that this scaling breaks down in the fixed temperature limit. Similarly, using (5.11) and (5.15) in (5.12) gives a lower bound on ΔT, and hence (via $Ra = R\Delta T$) on the Rayleigh number:

$$Ra \geq \widetilde{\mathcal{R}}_{a,\eta}(R) = R\,\widetilde{\mathcal{D}}_{a,\eta}(R) \sim 3 \times 2^{-1} \left(2 + \eta^{-1}\right)^{2/3} R^{2/3}. \tag{5.17}$$

Finally, combining (5.16) and (5.17), the conservative analytical upper bound on the Nu-Ra scaling for $\eta > 0$, asymptotically for large Ra, is

$$Nu \lesssim 2^{1/2}\, 3^{-3/2}\, Ra^{1/2} \approx 0.272\, Ra^{1/2}. \tag{5.18}$$

Note that this bound is independent of Biot number $\eta > 0$, and coincides with that in the fixed flux case.

5.3.2 Conservative numerical bounds and their scaling

The semi-optimal bounds on the Nu-Ra relationship, computed as described in Section 4.2, are summarized in Figure 4. The bounds take the form $Nu \leq \overline{C}_\eta(Ra) Ra^{1/2}$, where for sufficiently large Ra, $\overline{C}_0(Ra) = C_0 \approx 0.045$ and $\overline{C}_\infty(Ra) = C_\infty \approx 0.078$. For any $\eta > 0$, we see that $\overline{C}_\eta(Ra) \to C_\infty$ as $Ra \to \infty$, while for any large enough finite Ra, for sufficiently small η the bounds behave as in the fixed temperature case, $\overline{C}_\eta(Ra) \to C_0$ as $\eta \to 0$. That is, the $Ra \to \infty$ and $\eta \to 0$ limits do not commute; fixed temperature BCs form a singular limit of this bounding problem [35].

As suggested by Figure 4, for small η we compute the transition Rayleigh number $Ra_t(\eta)$ (and the corresponding $R_t(\eta)$) as that for which $Nu/Ra^{1/2}$ has crossed halfway from the fixed temperature to the fixed flux limiting values: $\overline{C}_\eta(Ra_t(\eta)) = (C_0 + C_\infty)/2 \approx 0.0615$. We find the expected scaling, $Ra_t(\eta) \sim 221\, \eta^{-2}$, consistent with $Ra_t(\eta) \to \infty$ as $\eta \to 0$. We also find $\delta_c \approx 0.8\,\eta$ at $Ra = Ra_t(\eta)$, confirming that the transition occurs when δ and η are comparable.

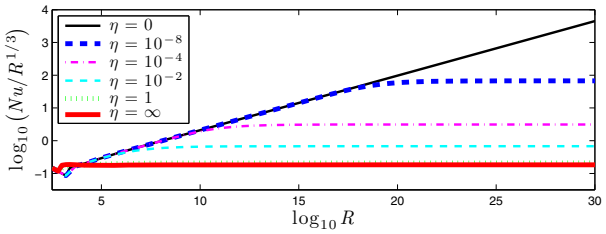

Fig. 5. (Color online) General Biot number BCs: the upper bound $\widetilde{\mathcal{N}}_\eta$ on the Nusselt number Nu, scaled by $R^{1/3}$, as a function of the control parameter R. For small $\eta > 0$, there is an extended "fixed temperature" regime where $\widetilde{\mathcal{N}}_\eta \sim \mathcal{O}(R^{1/2})$, but beyond a transition value $R_t(\eta) \sim \mathcal{O}(\eta^{-2})$ the fixed flux scaling $\widetilde{\mathcal{N}}_\eta \sim \mathcal{O}(R^{1/3})$ takes over.

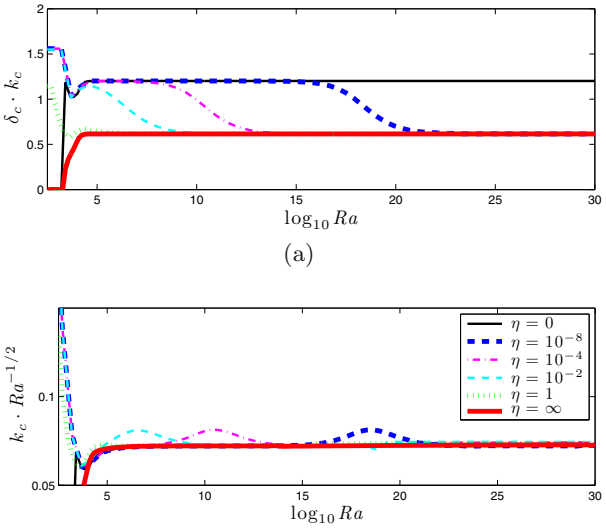

Fig. 6. (Color online) General Biot number BCs: (a) the computed $\delta_c k_c$ given as a function of $\widetilde{\mathcal{R}}_\eta$, the lower bound on Ra. (b) The critical wave number k_c, scaled by $\widetilde{\mathcal{R}}_\eta^{1/2}$, as a function of $\widetilde{\mathcal{R}}_\eta$; $k_c/\widetilde{\mathcal{R}}_\eta^{1/2}$ appears to have the same large-Ra asymptotic values in the fixed temperature and fixed flux limits.

The behaviour of the Nu bound with increasing control parameter R, shown in Figure 5, clearly reveals the distinct scaling regimes: for sufficiently small η, the bound scales initially as for fixed temperature, $Nu \leq C_0\, R^{1/2}$; but for $R \geq R_t(\eta)$, it takes the fixed flux scaling form $Nu \leq \widetilde{c}_\eta R^{1/3}$. The analytical bounds suggest investigating the dependence of the prefactor $\widetilde{c}_\eta$ on $2 + \eta^{-1}$; consistent with the analysis, we find $\widetilde{c}_\eta = \widetilde{c}(2 + \eta^{-1})^{1/3}$, where we compute $\widetilde{c} \approx 0.145$ (compare the analytical result $\widetilde{c} = 1/3$ (5.16)).

The numerically computed R_e and δ_c also scale as in the analytical bounds [38]. Figure 6 shows k_c, for which the uniform-in-k analysis makes no scaling predictions. For any $\eta > 0$, as usual we find the fixed flux value $\delta_c k_c \approx 0.6$ as $Ra \to \infty$, while for small η and small Ra, as for fixed

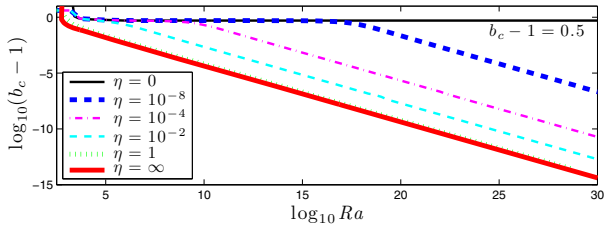

Fig. 7. (Color online) General Biot number BCs: the critical balance parameter b_c as a function of $\widetilde{\mathcal{R}}_\eta$, the lower bound on Ra. In the "fixed flux" scaling regime, we find $b_{c,\eta} - 1 \sim \mathcal{O}(\widetilde{\mathcal{R}}_\eta^{-1/2})$, and can write $b_{c,\eta} - 1 = c_\eta\, \delta_c$.

temperature BCs we have $\delta_c k_c \approx 1.2$. Interestingly, the asymptotic scaling of k_c with Ra does not appear to distinguish between $\eta = 0$ and $\eta > 0$; as seen in Figure 6b, while $k_c Ra^{1/2}$ increases slightly *during* the scaling transition, its large-Ra fixed flux and fixed temperature limits coincide.

The qualitative change in the behaviour of the balance parameter b in the $\eta = 0$ and $\eta = \infty$ limits, as discussed in Sections 5.1–5.2, is obvious in Figure 7. For $\eta \ll 1$, we see that $b_c \approx 3/2$ for $Ra < Ra_t(\eta)$, while for higher Ra, we have $b_c - 1 = \mathcal{O}(Ra^{-1/2})$. In this regime, we have $b_{c,\eta} - 1 \sim c_\eta\, \delta_c$, where we compute $c_\eta = 0.25\,(2 + \eta^{-1})$, coinciding with the analytical result (5.15).

6 Discussion

In Rayleigh-Bénard convection with highly, but not perfectly, conducting bounding plates, with dimensionless Biot number $0 < \eta \ll 1$, the bounding calculations reveal a clear transition in scaling: for small thermal driving, the system behaves as if the plates were perfect conductors, corresponding to fixed temperature BCs; while above a transition Rayleigh number $Ra_t(\eta)$, the bounds scale as if the plates were effectively insulating, in which case fixed flux conditions would be appropriate.

It is tempting to wonder whether this bounding transition reflects any observable changes in the statistics of the connectively turbulent fluid. We note, though, that the transition occurs when the parameter δ, a proxy for the thermal boundary layer thickness, is comparable to η; equivalently, when $Nu \approx \mathcal{O}(\eta^{-1})$. For highly conducting boundaries any transition is thus likely to be beyond the reach of experiment or direct numerical simulation. Furthermore, recent computational studies have been unable to distinguish between properties of fixed flux and fixed temperature high-Ra Rayleigh-Bénard convection [32].

The evidence regarding whether, and how, the thermal BCs influence properties of turbulent convection for high Ra thus seems to be inconclusive. Any potential effect of the thermal characteristics of the boundaries is also, to date, unknown for flows other than finite Prandtl number Rayleigh-Bénard convection (for example, analytical bounds on convective heat transfer with fixed flux BCs [25] have not, to our knowledge, been successfully derived for porous medium convection [22]).

Using piecewise linear background profiles $\tau_\delta(z)$, we have obtained bounds on heat transport in finite Prandtl number Rayleigh-Bénard convection for mixed thermal BCs of general Biot number $0 \le \eta \le \infty$, both by using elementary analytical estimates uniform in wave number, and by numerically optimizing over all such profiles using the method developed by Otero [18]. We find that the bounds all take the form $Nu \le C_\eta\, Ra^{1/2}$, where in the large-Ra limit, $C_\eta = C_\infty$ for any $\eta > 0$. As expected, the numerical optimization improves the prefactor: from $C_0 = 3\sqrt{6}/32 \approx 0.23$ to 0.045 for fixed temperature boundaries, and from $C_\infty = \sqrt{2/27} \approx 0.272$ to 0.078 for fixed flux and general thermal BCs. For $\eta > 0$, these bounds improve on previous results [25,35] for imperfectly conducting plates.

We observe that the computed asymptotic bounds on the Nu-Ra relationship are lower for fixed temperature BCs, corresponding to perfectly conducting boundaries, than for perfectly insulating or more general imperfectly conducting plates. It remains to be seen whether this holds true also for the best upper bounds, optimizing over all background profiles $\tau(z)$ rather than merely over a one-parameter piecewise linear family.

Indeed, a fundamental open question here is whether for fixed flux or general BCs, the optimal scaling exponent over all admissible backgrounds $\tau(z)$ in a bound of the form $Nu \le C\, Ra^p$ remains $p = 1/2$, as it does in the fixed temperature case. In this regard the example of infinite Prandtl number convection (with fixed temperature BCs) is instructive: the standard background method using the one-parameter family $\tau_\delta(z)$ yielded an analytical bound of the form $Nu \le CRa^p$ with $p = 2/5$ [21], and this scaling was confirmed by the semi-optimal numerical solution for such backgrounds [18]. However, the lower exponent $p = 1/3$ was suggested by calculations using the MHB bounding approach [42], and by a rigorous bound obtained outside the CDH background field formalism [43]. That the background method could also yield lower scaling exponents in this problem was shown numerically by Plasting and Ierley [16], who extended Otero's method to a two-parameter family of piecewise linear backgrounds $\tau(z)$ in which the interior gradient τ' was allowed to be nonzero, and found a high-Ra scaling of the resultant conservative bounds consistent with $p = 7/20$. Indeed, an improved analytical bound for infinite Prandtl number flow using the background method has since been found: using a field $\tau(z)$ with a logarithmic, stably stratified profile in the bulk of the fluid, Doering et al. [44] have proved $Nu \le CRa^{1/3}(\ln Ra)^{1/3}$.

Finally, we remark that Rayleigh-Bénard convection with imperfectly conducting boundaries may be modelled more realistically by considering a horizontal fluid layer in contact above and below with plates of dimensionless finite thickness d and conductivity λ (scaled relative to the corresponding fluid quantities). Bounds on heat transport may also be obtained for this system [35]; at the level of conservative analyses for piecewise linear backgrounds, they coincide with those for mixed thermal BCs with Biot number $\eta = d/\lambda$.

We would like to thank Charlie Doering and David Muraki for helpful discussions, and the IRMACS Centre at Simon Fraser University for providing a productive research environment. This work was partially supported by grants from NSERC.

References

1. L.P. Kadanoff, Phys. Today **54**, 34 (2001)
2. G. Ahlers, Physics **2**, 74 (2009)
3. G. Ahlers, S. Grossmann, D. Lohse, Rev. Mod. Phys. **81**, 503 (2009)
4. M.V.R. Malkus, Proc. Roy. Soc. Lond. A **225**, 196 (1954)
5. L.N. Howard, J. Fluid Mech. **17**, 405 (1963)
6. L.N. Howard, Ann. Rev. Fluid Mech. **4**, 473 (1972)
7. F.H. Busse, J. Fluid Mech. **37**, 457 (1969)
8. F.H. Busse, Adv. Appl. Mech. **18**, 77 (1978)
9. N.K. Vitanov, Eur. Phys. J. B **73**, 265 (2010)
10. E. Hopf, Math. Ann. **117**, 764 (1941)
11. C.R. Doering, P. Constantin, Phys. Rev. Lett. **69**, 1648 (1992)
12. C.R. Doering, P. Constantin, Phys. Rev. E **49**, 4087 (1994)
13. C.R. Doering, P. Constantin, Phys. Rev. E **53**, 5957 (1996)
14. R.R. Kerswell, Physica D **121**, 175 (1998)
15. R.R. Kerswell, Phys. Fluids **13**, 192 (2001)
16. S.C. Plasting, G.R. Ierley, J. Fluid Mech. **542**, 343 (2005)
17. P. Constantin, C.R. Doering, Physica D **82**, 221 (1995)
18. J. Otero, Ph.D. thesis, University of Michigan, 2002
19. S.C. Plasting, R.R. Kerswell, J. Fluid Mech. **477**, 363 (2003)
20. G.R. Ierley, R.R. Kerswell, S.C. Plasting, J. Fluid Mech. **560**, 159 (2006)
21. C.R. Doering, P. Constantin, J. Math. Phys. **42**, 784 (2001)
22. C.R. Doering, P. Constantin, J. Fluid Mech. **376**, 263 (1998)
23. J. Otero, L.A. Dontcheva, H. Johnston, R.A. Worthing, A. Kurganov, G. Petrova, C.R. Doering, J. Fluid Mech. **500**, 263 (2004)
24. R. Nicodemus, S. Grossmann, M. Holthaus, Physica D **101**, 178 (1997)
25. J. Otero, R.W. Wittenberg, R.A. Worthing, C.R. Doering, J. Fluid Mech. **473**, 191 (2002)
26. S. Chaumat, B. Castaing, F. Chillà, *Rayleigh-Bénard cells: influence of the plates' properties*, in *Advances in Turbulence IX, Proceedings of the Ninth European Turbulence Conference*, edited by I.P. Castro, P.E. Hancock, T.G. Thomas (CIMNe, Barcelona, 2002), pp. 159–162
27. F. Chillà, M. Rastello, S. Chaumat, B. Castaing, Phys. Fluids **16**, 2452 (2004)
28. E. Brown, A. Nikolaenko, D. Funfschilling, G. Ahlers, Phys. Fluids **17**, 075108 (2005)
29. R. Verzicco, Phys. Fluids **16**, 1965 (2004)
30. J.J. Niemela, K.R. Sreenivasan, J. Fluid Mech. **557**, 411 (2006)
31. G. Ahlers, D. Funfschilling, E. Bodenschatz, New J. Phys. **11**, 123001 (2009)
32. H. Johnston, C.R. Doering, Phys. Rev. Lett. **102**, 064501 (2009)
33. R. Verzicco, K.R. Sreenivasan, J. Fluid Mech. **595**, 203 (2008)
34. R.J.A.M. Stevens, R. Verzicco, D. Lohse, J. Fluid Mech. **643**, 495 (2010)
35. R.W. Wittenberg (2010), to appear in J. Fluid Mech.
36. D.D. Joseph, *Stability of Fluid Motions* (Springer-Verlag, New York, 1976)
37. D.T.J. Hurle, E. Jakeman, E.R. Pike, Proc. R. Soc. London A **296**, 469 (1967)
38. J. Gao, Master's thesis, Simon Fraser University, 2006
39. A. Pellew, R.V. Southwell, Proc. R. Soc. A **176**, 312 (1940)
40. R. Nicodemus, S. Grossmann, M. Holthaus, J. Fluid Mech. **363**, 281 (1998)
41. E.M. Sparrow, R.J. Goldstein, V.K. Jonsson, J. Fluid Mech. **18**, 513 (1964)
42. S.K. Chan, Stud. Appl. Math. **50**, 13 (1971)
43. P. Constantin, C.R. Doering, J. Stat. Phys. **94**, 159 (1999)
44. C.R. Doering, F. Otto, M.G. Reznikoff, J. Fluid Mech. **560**, 229 (2006)